FINAL PUBLISHABLE REPORT

Grant Agreement number	17IND11
Project short name	Hi-TRACE
Project full title	Industrial process optimisation through improved metrology of thermophysical properties

Project start date and duration:		01 July 2018, 42 months
Coordinator: Bruno Hay, LNE Tel: +33 1 30 69 12 20 E-mail: bruno.hay@lne.fr Project website address: www.hi-trace.eu		
Internal Funded Partners: 1 LNE, France 2 NPL, UK 3 PTB, Germany 4 VINS, Serbia	External Funded Partners: 5 ArianeGroup, France 6 CEA, France 7 FHWS, Germany 8 JRC, Europe 9 TUG, Austria 10 ZAE, Germany	Unfunded Partners: 11 NETZSCH, Germany
RMG: -		

This publication reflects only the author's view and the Commission is not responsible for any use that may be made of the information it contains.

The EMPIR initiative is co-funded by the European Union's Horizon 2020 research and innovation programme and the EMPIR Participating States

TABLE OF CONTENTS

1 Overview

Many industries such as space, aeronautics, nuclear energy and glass, operate installations at temperatures above 1500 °C. In order to optimise their processes and increase their competitiveness, these industries develop new materials able to work at higher temperatures. The overall objective of this project was to establish a European metrological infrastructure composed of reference facilities in order to provide industries with reliable and accurate thermophysical properties data for solid material up to 3000 °C.

The project has developed or has improved methods and equipment for the measurements of thermophysical properties at ultra-high temperatures and demonstrated their metrological capabilities through the thermal characterization of several refractory materials. Reference facilities are now accessible to industry at consortium partner organisations and datasets with high temperature thermal diffusivity, specific heat, and spectral emissivity values of the materials studied during the project are available in the Zenodo open access repository.

2 Need

Over recent years, the operational temperatures of process plants or components in safety-critical applications have been increased, e.g., above 1500 °C.

- In space applications, space modules need reliable thermophysical properties data (thermal diffusivity, specific heat, emissivity and temperature of fusion) at temperatures as high as 2500 °C, for optimising re-entry vehicle designs. ArianeGroup has shown, for example, that numerical models may overestimate the temperature of the shield of re-entry vehicles by 600 °C. Adapted models and accurate thermophysical properties data are necessary to achieve a better prediction.
- In nuclear applications, the use of current zirconium-based alloys is very common for manufacturing fuel cladding. Silicon carbide based composite materials are seen today as one promising alternative for the use of Accident Tolerant Fuel cladding applications, as their oxidation temperature is far higher than that of zirconium-based alloys (approximately 2000 °C vs 1200 °C). Knowing the thermal diffusivity and specific heat of these 3D fibre reinforced composite materials is crucial for predicting their behaviour in industrial conditions.
- In gas turbines, many design factors influence the overall efficiency, but a major step has been achieved by increasing the engine temperature by 7 % when using thermal barrier coatings. However, for these coatings the state of bonding (which influences the thermal resistance between interfaces) is very critical for their operability, as the materials are used close to their temperature limit. A discrepancy of a few degrees significantly changes the operability of a gas turbine.

In the examples mentioned above, no traceable thermophysical properties measurements existed at very high temperatures (above 1500 °C) for assessing uncertainties of the measured values. In order to fill this gap, it was needed to have reference facilities based on absolute measurement methods with their corresponding uncertainty budgets.

3 Objectives

The aim of the project was to increase the traceability to the SI of thermophysical properties measurements at very high temperature through reference facilities, new set-ups, calibration methods, uncertainty budgets and reference materials.

The specific objectives of Hi-TRACE project were:

1. To establish a reference facility based on the laser flash method for traceable measurement of thermal diffusivity of solid materials between 1500 °C and 3000 °C and to determine the related uncertainty budget.
2. To develop validated methods and establish reference facilities (based on drop calorimetry or laser flash method) for the traceable measurement of specific heat of solid materials between 1500 °C and 3000 °C. The target uncertainty was 0.5 % below 1000 °C and 1.5 % above.
3. To establish a reference facility for the traceable measurement of emissivity of solid materials above 1500 °C based on radiometric or calorimetric methods. The target uncertainty was 0.5 % below 1000 °C

and 1.5 % above. In addition, to develop validated methods for the measurement of the melting temperature of materials up to 3000 °C.

4. To develop validated methods to quantify the mechanical adhesion of solid materials, in particular functional layers, for thermal or corrosion protection above 1000 °C via the thermal contact resistance.
5. To facilitate the take up of the technology and measurement infrastructure developed in the project by standards developing organisations and end-users.

4 Results

4.1 *Objective 1: Establishing traceability for thermal diffusivity measurements at temperatures up to 3000 °C*

Some academic laboratories or companies perform thermal diffusivity measurements of solid materials at very high temperature by using commercial devices operating up to 2800 °C. Before this project, the traceability of these measurements to the SI could not be guaranteed above 2000 °C due to the limitation of reference facilities available in NMIs.

A reference laser flash apparatus (LFA) has been improved in this project to address this issue by enabling traceable measurement of thermal diffusivity of solid materials at temperatures up to 3000 °C. The uncertainty budgets associated to these measurements have been established for three refractory materials (isotropic graphite, molybdenum and tungsten). The variability and coherency of very high temperature thermal diffusivity measurements performed at the European level have been assessed through a comparison of the facilities used by the partners (ArianeGroup, CEA, FHWS, NETZSCH, NPL, TUG and VINCA) with the reference LFA of LNE.

4.1.1 Development of a reference facility for measuring the thermal diffusivity up to 3000 °C

LNE has performed for many years thermal-diffusivity measurements of homogeneous solid materials up to 2000 °C in inert or vacuum environments by using a homemade facility based on the well-known principle of the rear face laser-flash method [1]. In this method, a cylindrical specimen is heated on its front face by a short energy pulse, and the induced transient temperature rise versus time is measured on its back face. The thermal diffusivity is determined with an estimation procedure based on minimizing the difference between the experimental temperature-time curve (thermogram) and the same curve given by a theoretical model of the transient heat conduction through the specimen. In the case of a bulk homogeneous material, the thermal diffusivity is estimated by LNE according to the *partial time moments method* [2].

In its former configuration, this facility was equipped with two furnaces, a resistive furnace operating from room temperature to 800 °C and an inductive one for the measurements performed from 700 °C to 2000 °C. This set-up has been extensively modified to enable the measurement of the thermal diffusivity of solid materials up to 3000 °C. A schematic representation of this new facility is shown in Figure 1-a.

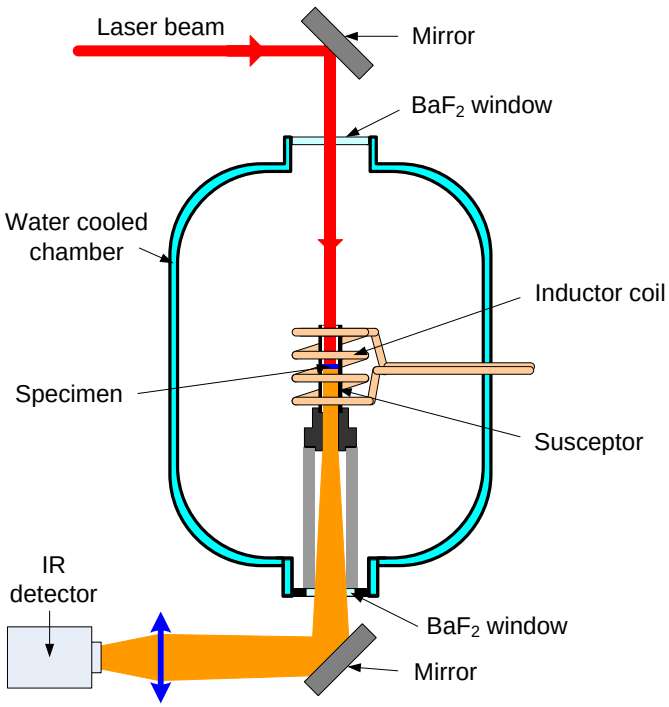

a) Schematic diagram of the diffusivimeter of LNE

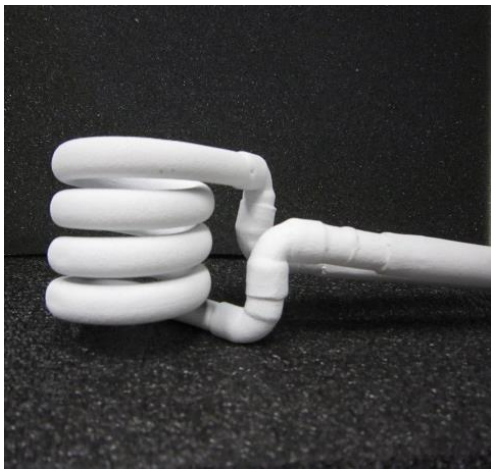

b) Inductive coil

Figure 1 - LNE facility for the thermal diffusivity measurement of solid materials up to 3000 °C

The specimen (disk of 10 mm in diameter and 1 mm to 4 mm thick) is maintained at a constant temperature in the inductive furnace composed by an airtight water cooled enclosure in the centre of which an inductive coil and a movable susceptor are placed on a vertical axis. The inductive coil is a copper solenoid also cooled by circulating water and connected to a 50 kW high frequency generator (100 kHz to 400 kHz). Its geometry has been optimised (reduction of the number of turns from 5 to 4 to increase the distance between each turn and coating of the coil with a ceramic deposit) in order to avoid the appearance of sparks between the susceptor and the coil as well as sparks between the turns themselves that can damage the susceptor and disturb the measurements. Figure 1-b presents a picture of the new copper induction coil with the ceramic coating.

The susceptor is a hollow cylinder having a shoulder machined at mid-height to maintain the specimen. The Foucault currents (also named eddy currents) induced in the susceptor generate heat by Joule heating, the specimen located inside being then heated primarily by radiative transfer. Depending on the temperature range and the material of the specimen, a thin washer made of molybdenum or tungsten is put between the specimen and the graphite susceptor in order to avoid any direct contact between them with the objective to limit chemical interactions at high temperature. The geometry of the susceptor has been modified and the diameter of its support has been reduced in order to limit conduction heat losses. The cooling loop of the inductive coil and of the enclosure has been improved in order to both increase the cooling efficiency and to reduce the temperature variations of the enclosure wall from 29 °C $\pm$ 2 °C to 29 °C $\pm$ 0.3 °C.

Two power supplies have been implemented in the high frequency generator of the inductive furnace in order to optimize the temperature resolution depending on the level of temperature: a 25 kW configuration to enable 2800 °C to be reached with a temperature resolution of 12 °C at 1000 °C and 1 °C at 2800 °C, and a 50 kW configuration for higher temperatures, with temperature resolution of 25 °C at 1000 °C and 2 °C at 3000 °C. A filter has been put at the output of the HF generator to reduce the high frequency electromagnetic interferences (> 250 kHz). These modifications enable to increase the signal to noise ratio and therefore to obtain exploitable thermograms up to 3000 °C. The furnace is equipped with two BaF_2 windows, which are transparent (transmission higher than 90% from 0.25 µm up to 10 µm) at the laser wavelength and in the wavelength ranges of the IR detectors.

The temperature of the specimen is measured during heating of the furnace as well as when temperature is stabilized at target temperature with one of the two infrared bi-chromatic radiation thermometers (0.90 µm and 1.05 µm) operating in the temperature ranges [700 °C - 1800 °C] or [1000 °C - 3000 °]. They are installed on a linear stage enabling to put one or the other opposite the 90° flat mirror attached below the movable susceptor. These radiation thermometers can be subjected to drift along time and need thus to be periodically calibrated to ensure trueness of temperature measurements. A specific protocol, based on the use of metal-carbon eutectic high temperature fixed points positioned in the furnace at the location of the specimens, has been developed at LNE in order to enable the *in situ* calibration of the radiation thermometers. The eutectic fixed points are palladium-carbon (1492 °C), platinum-carbon (1738 °C) and iridium-carbon (2290 °C).

The short thermal excitation (duration around 450 µs) is generated by a Nd:phosphate glass laser at 1054 nm wavelength, whose beam is shaped by a set of lenses, mirrors and stops so that its diameter is about 10 mm on the front face of the specimen. A photodiode is used to measure the duration, the temporal profile of the pulse, and the time origin that corresponds to the time when the laser beam irradiates the specimen. The induced transient temperature rise of the specimen rear face is measured optically with an infrared detector (HgCdTe, InGaAs and Si depending on the temperature range). An optical system made of lenses is associated to each IR detector in order to collect the infrared radiation emitted by the specimen rear face.

4.1.2 Assessment of uncertainty on very high temperature thermal diffusivity measurements

a) Expanded uncertainty (k=2) on thermal diffusivity measurements estimated by all partners

The uncertainties associated to thermal diffusivity measurements performed at high temperature on isotropic graphite, molybdenum and tungsten have been estimated for the different LFA involved in the inter-laboratory comparison presented in section 4.1.3.

Table 1 summarize the expanded uncertainties (*k=2*) assessed by the participant laboratories, assuming that the thickness used for the determination of the thermal diffusivity is corrected by the thermal expansion of the tested material.

An example of assessment of an uncertainty budget is presented in the following pages in the case of the laser flash facility of LNE.

Table 1 - Expanded uncertainty associated with thermal diffusivity measurements

Temp. level	Expanded Uncertainty (*k=2*) [%]												
[°C]	AGS	CEA	FHWS	LNE			Netzsch	NPL			VINCA		
Material	All	All	All	IG210	W	Mo	All	IG210	W	Mo	IG210	W	Mo
20	4.0	5.0	5.0	3.2	3.5	3.5	3.0	5.0	4.0	6.8	4.8	1.8	1.6
50	4.0	5.0	5.0	3.2	3.5	3.5	3.0	5.0	5.0	4.4			
100	4.0	5.0	5.0	3.1	3.4	3.4	3.0	4.0	3.6	4.2		1.8	1.4
150	4.0	5.0	5.0	3.1	3.4	3.4	3.0	3.8	3.4	4.2			
200	4.0	5.0	5.0	3.1	3.4	3.4	3.0	3.8	3.4	4.4	3.2	2.0	1.6
250	4.0	5.0	5.0	3.0	3.3	3.3	3.0	3.6	3.4	4.4			
300	4.0	5.0	5.0	3.0	3.2	3.2	3.0	3.6	3.4	4.4		1.6	
400		5.0	5.0	3.0	3.2	3.2	3.0	3.6	3.4	4.2	1.4	1.4	1.4
600		5.0	5.0	3.0	3.3	3.3	3.0	3.6	3.6	3.8	1.8	1.6	1.2
800		5.0	5.0	3.1	3.5	3.5	3.0	3.6	4.4	3.4	1.2	1.6	1.2
1000		5.0	5.0	3.1	3.7	3.7	3.0	4.2	3.4	3.8	1.2	1.8	1.6
1200		5.0	5.0	3.3	3.7	3.7	3.0	4.4	5.2	3.6	2.8	3.0	2.8
1400		5.0	5.0	3.4	3.8	3.8	3.0	4.4	4.6	3.8			
1600		5.0	5.0	3.7	3.9	3.9	3.0						
1800		5.0	5.0	3.7	4.0	4.0	3.0						
2000			5.0	3.8	4.2	4.2	3.0						
2200			5.0	4.0	4.6	4.7	3.0						
2400			5.0	4.2	5.0		3.0						
2600			5.0	4.3			3.0						
2800			5.0	4.4			3.0						
3000				4.7									

b) Uncertainty on thermal diffusivity measured by LFA at LNE

The thermal diffusivity is determined by identification of the experimental thermogram with a theoretical model, which is in the classical case of a homogeneous material a two-parameter unidirectional model depending on the thermal diffusivity a and the dimensionless Biot number Bi. This analytical model is obtained by solving the heat conduction equation for the case of a homogeneous, isotropic and opaque specimen assuming that ① the model is linear (thermophysical properties are considered independent of the temperature), ② the heat losses between the sample and its surrounding are characterized by a uniform and constant in time heat-exchange coefficient, ③ the laser pulse is spatially uniform and can be considered as a Dirac pulse.

In the *partial time moments method*, the thermal diffusivity is estimated from the partial time moments of order 0 and -1 determined for the experimental and theoretical thermograms *f(t)* normalized by their *maxima* (Figure 2 presents an example of such a thermogram). The experimental (m_0 and m_{-1}) and theoretical (m_0^* and m_{-1}^*) partial time moments are written in a general way as follows, where $t_{0.1}$ and $t_{0.8}$ correspond to the times needed for the back face of the specimen to reach respectively 10 % and 80 % of the maximum amplitude of the thermogram:

$$m_0 = \int_{t_{0.1}}^{t_{0.8}} f(t)dt \quad \text{and} \quad m_{-1} = \int_{t_{0.1}}^{t_{0.8}} f(t)/t\, dt \tag{1}$$

The theoretical and experimental partial time moments are linked by the two following relationships where *e* is the specimen thickness:

$$m_0 = m_0^* \cdot e^2/a \quad \text{and} \quad m_{-1} = m_{-1}^* \tag{2}$$

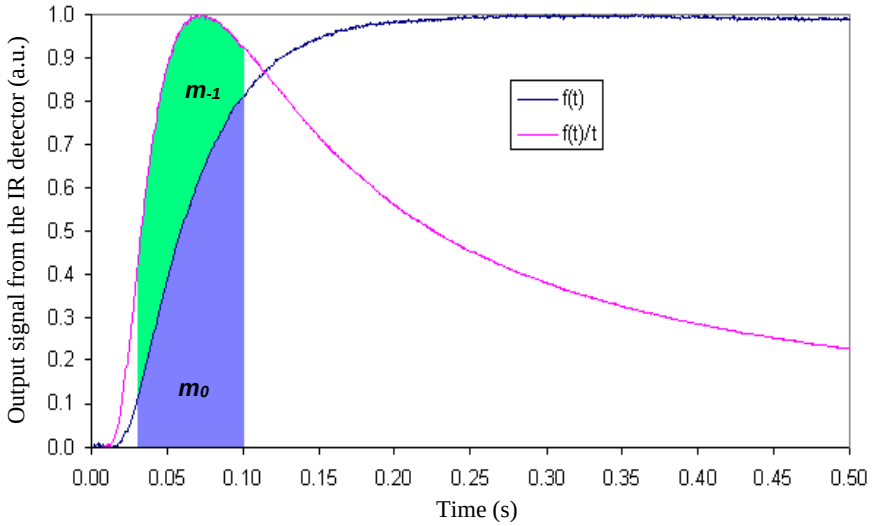

Figure 2 - Example of experimental thermogram

A relation between the theoretical moments m_0^* and m_{-1}^*, named identification function *F*, is established by a polynomial fit of couples of values (m_0^* , m_{-1}^*) calculated from thermograms obtained for various values of *Bi* using the analytical model. The coefficients b_i depend on the geometrical ratio *R/e* of the specimen (where *R* is the radius of the specimen).

$$m_0^* = F(m_{-1}^*) = \sum_{i=0}^{n} b_i \cdot (m_{-1})^i \tag{3}$$

The thermal diffusivity a is then given by the following relationship by combining equations 2 and 3:

$$a = F(m_{-1}) \cdot e^2 / m_0 \tag{4}$$

The analytical expression of the variance $u^2(a)$ is determined by applying the propagation law of variances to the mathematical model given by equation 4, assuming that the partial time moments m_0 and m_{-1} are correlated together and are not dependent on the thickness *e* and on the identification function coefficients b_i. The coefficients b_i are assumed to be correlated together and not dependent on the thickness *e*.

$$u^2(a) = c_{m_0}^2 \cdot u^2(m_0) + c_{m_{-1}}^2 \cdot u^2(m_{-1}) + 2 \cdot c_{m_0} \cdot c_{m_{-1}} \cdot u(m_0, m_{-1}) + c_e^2 \cdot u^2(e) + c_F^2 \cdot u^2(F) + u^2(\bar{a}) + u_{hyp}^2(a) + u_T^2(a) \tag{5}$$

with

$$c_e = 2 \cdot e \cdot \sum_{i=0}^{n} b_i \cdot m_{-1}^i / m_0 \qquad c_F = e^2 / m_0$$

$$c_{m_0} = -e^2 \cdot \sum_{i=0}^{n} b_i \cdot m_{-1}^i / m_0^2 \qquad c_{m_{-1}} = e^2 \cdot \sum_{i=1}^{n} i \cdot b_i \cdot m_{-1}^{i-1} / m_0$$

The uncertainty on thermal diffusivity results from the combination of the standard uncertainties on the calculation of the partial time moments $u(m_0)$ and $u(m_{-1})$, on the thickness determination $u(e)$, on the establishment of the identification function $u(F)$, on the measurement process $u(\bar{a})$ and $u_{hyp}(a)$, and on the measurement of the specimen temperature $u_T(a)$. The uncertainty factor $u(\bar{a})$ is linked to the determination of the thermal diffusivity value from the repeatability of three consecutive measurements. The term $u_{hyp}(a)$ is due to the use of the function *F* for experimental conditions different from the assumptions for which it was determined. The uncertainty $u_T(a)$ corresponds to the uncertainty on the thermal diffusivity due to the uncertainty on the test temperature *T*. Table 2 gives an example of uncertainty budget evaluated in the case of the measurement of thermal diffusivity of isotropic graphite at 3000 °C. More details can be found in [3].

LNE has estimated the relative expanded uncertainty associated with the thermal diffusivity determination between 3 % and 5 % for the three refractory materials in the whole temperature range, if the thermal expansion of the tested specimens is corrected.

Table 2 Uncertainty budget associated with thermal diffusivity value measured on isotropic graphite at 3000 °C

Uncertainty component	Value	Standard uncertainty (k=1) or covariance	Sensitivity coefficient	Contribution(1)
X_i	x_i	$u(x_i)$ or $u(x_i,x_j)$	$\partial a / \partial X_i$	(%)
Partial time moment m_{-1}	0.3975	3.05×10^{-3}	4.61×10^{-5} m^2·s^{-1}	61.2
Partial time moment m_0	0.0506 s	3.40×10^{-4} s	-1.52×10^{-4} m^2·s^{-2}	8.3
Covariance factor $u(m_0, m_{-1})$	0	2.43×10^{-9} s	-1.40×10^{-8} m^4·s^{-3}	-0.1
Thickness e	3.055×10^{-3} m	3.67×10^{-6} m	5.02×10^{-3} m·s^{-1}	1.1
Identification function F	0.04161	2.24×10^{-4}	1.84×10^{-4} m^2·s^{-1}	5.3
Theoretical assumptions	0	5.81×10^{-8} m^2·s^{-1}	1	10.5
Average of 3 measurements	7.62×10^{-6} m^2·s^{-1}	4.62×10^{-8} m^2·s^{-1}	1	6.6
Specimen temperature T	2985 °C	15.2 °C	3.14×10^{-9} m^2·s^{-1}·°C^{-1}	7.1

Thermal diffusivity a	Standard uncertainty	Expanded uncertainty (k=2)	
7.67×10^{-6} m^2·s^{-1}	1.79×10^{-7}m^2·s^{-1}	3.58×10^{-7}m^2·s^{-1}	4.7 %

(1) *The values expressed in % correspond to the contributions of each uncertainty component in terms of variance with respect to the total variance on the thermal diffusivity a.*

4.1.3 Inter-laboratory comparison on high temperature thermal diffusivity measurements

The specimens needed for this comparison have been machined by LNE in the same blocks of molybdenum, tungsten and isotropic graphite, in order to reduce any potential scattering of results between partners due to inhomogeneity effects. Before starting the inter-laboratory comparison, the homogeneity of the three batches of specimens has been checked by LNE through thermal diffusivity measurements performed at room temperature for three different thicknesses (1 mm, 2 mm and 3 mm). The results showed that the materials could be considered as homogeneous, with standard deviations lower than 1 % for molybdenum and tungsten, and lower than 1.5 % for the isotropic graphite IG210.

Thermal diffusivity measurements have been then performed by the partners (ArianeGroup, CEA, FHWS, LNE, NETZSCH, NPL, TUG and VINCA) up to the maximum temperatures that can be reached by the facilities used and that are compatible with the tested materials (in terms of melting temperature and contamination). In order to examine potential aging effect, each specimen has been measured during two successive runs in the whole investigated temperature range with a final thermal diffusivity measurement at 23 °C after the second run.

Figure 3 shows as example the thermal diffusivity results versus temperature obtained by the participants during two successive heating runs for the isotropic graphite. For a better readability, Figure 4 presents for each temperature the relative deviations between the data obtained by the partners and the mean value determined from all results. The relative deviations observed for the results obtained by the participants at the highest temperatures (above 500 °C) were lower than ± 4 % for molybdenum, lower than ± 5 % for IG210 graphite and up to ± 9 % for the tungsten. The deviations observed between the results from AGS and those obtained by the other partners for these three materials have been explained after analysis by a malfunction of their facility during the measurement campaign.

The relative deviations observed between results obtained during the 1st and 2nd runs were lower than ± 3 % for the three materials (excepted for 8 data among 250 values of relative deviation). This proves the stability of the materials and the specimens, as these relative variations are within the measurement uncertainties estimated by the participants.

The potential influence of the heating mode (resistive or inductive) and of the materials used for the sample holders, which vary depending on the participants, has been scrutinized. The various heating configurations applied could lead indeed to disparities in the thermal cycling supported by the specimens (with strong differences of heating and cooling rates) and in the potential contamination of the specimens by the sample holders.

The thermal diffusivity measurements appeared to be insensitive to the heating method as no systematic trend (either higher or lower) were observed for results obtained with resistive heating compared to those obtained with inductive heating. It was also demonstrated that the choice of the sample holder had no strong influence on the results.

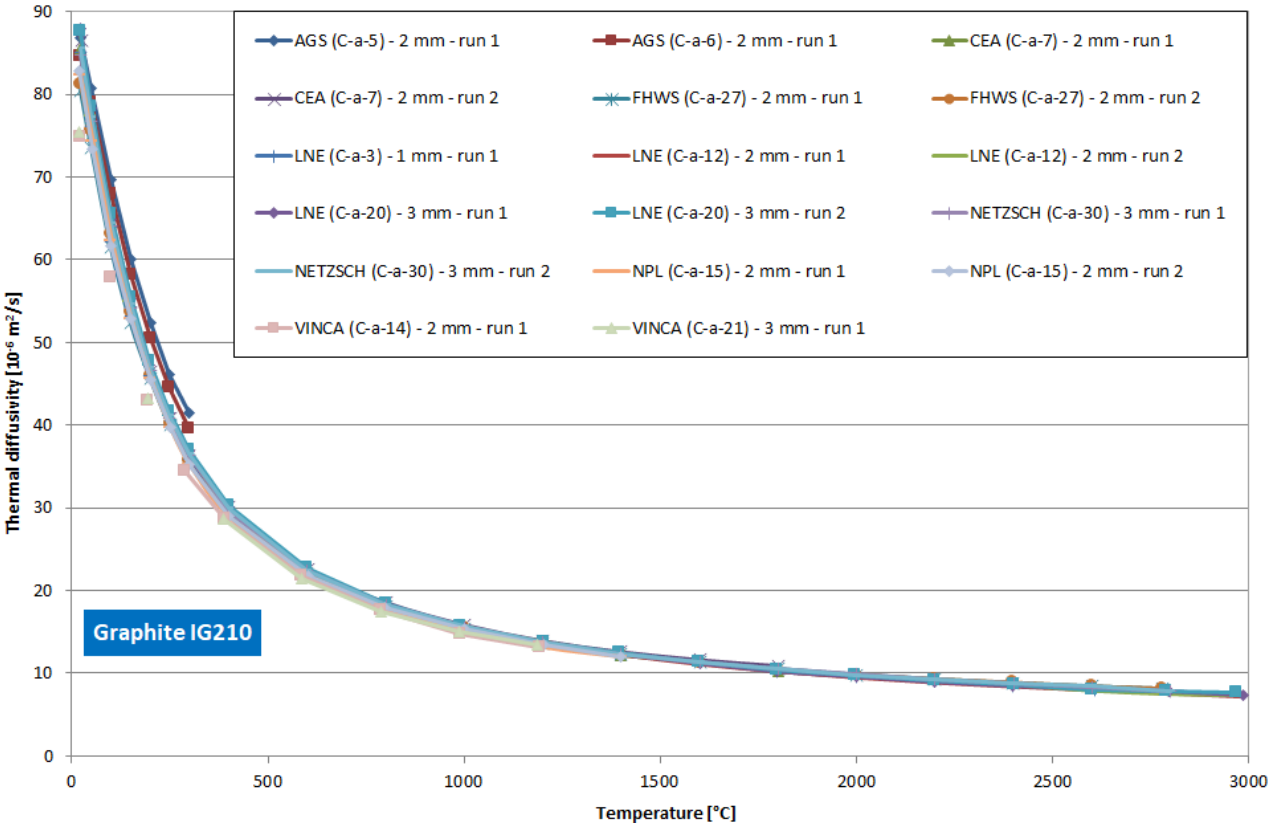

Figure 3 - Isotropic graphite IG210 - Thermal diffusivity measurements from 23 °C to 3000 °C

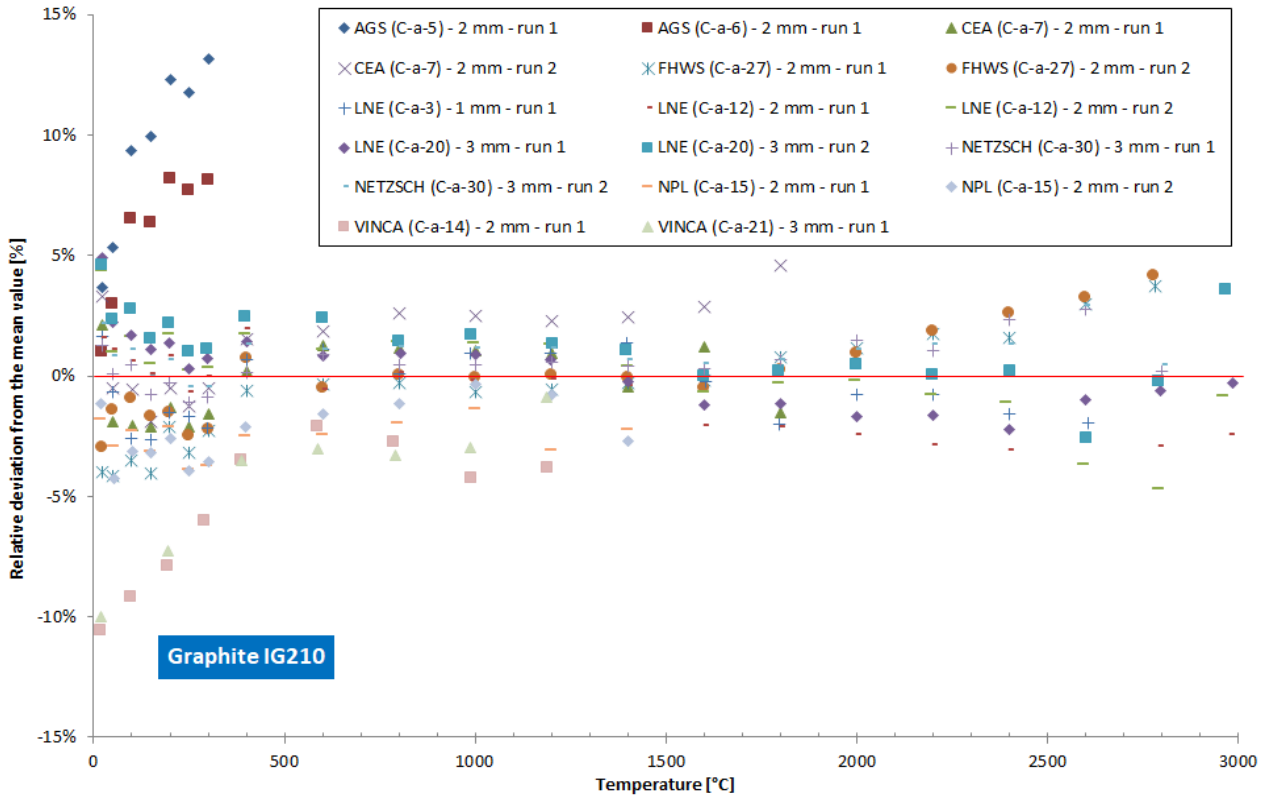

Figure 4 - Isotropic graphite IG210 - Relative deviations from the mean value

4.1.4 Application to the study of metallic alloys and composite materials

The LFA used in this inter-laboratory comparison were successfully applied in the last part of the project to measure the thermal diffusivity of “industrial” materials (composites and metallic alloys) at very high temperature. These materials, a TZM alloy (titanium-zirconium-molybdenum) and two C/SiC and SiC/SiC composite materials were provided by the industrial partners involved in the project or in the stakeholder advisory board.

A first analysis of the results shows deviations between the thermal diffusivity data obtained by the partners at the highest temperatures limited to ± 6 % for TZM alloy (cf. Figure 5). However, these relative deviations can be higher than ± 25 % in some cases for the C/SiC and SiC/SiC composite materials due to their inhomogeneity and to the modification of their microstructure during the tests.

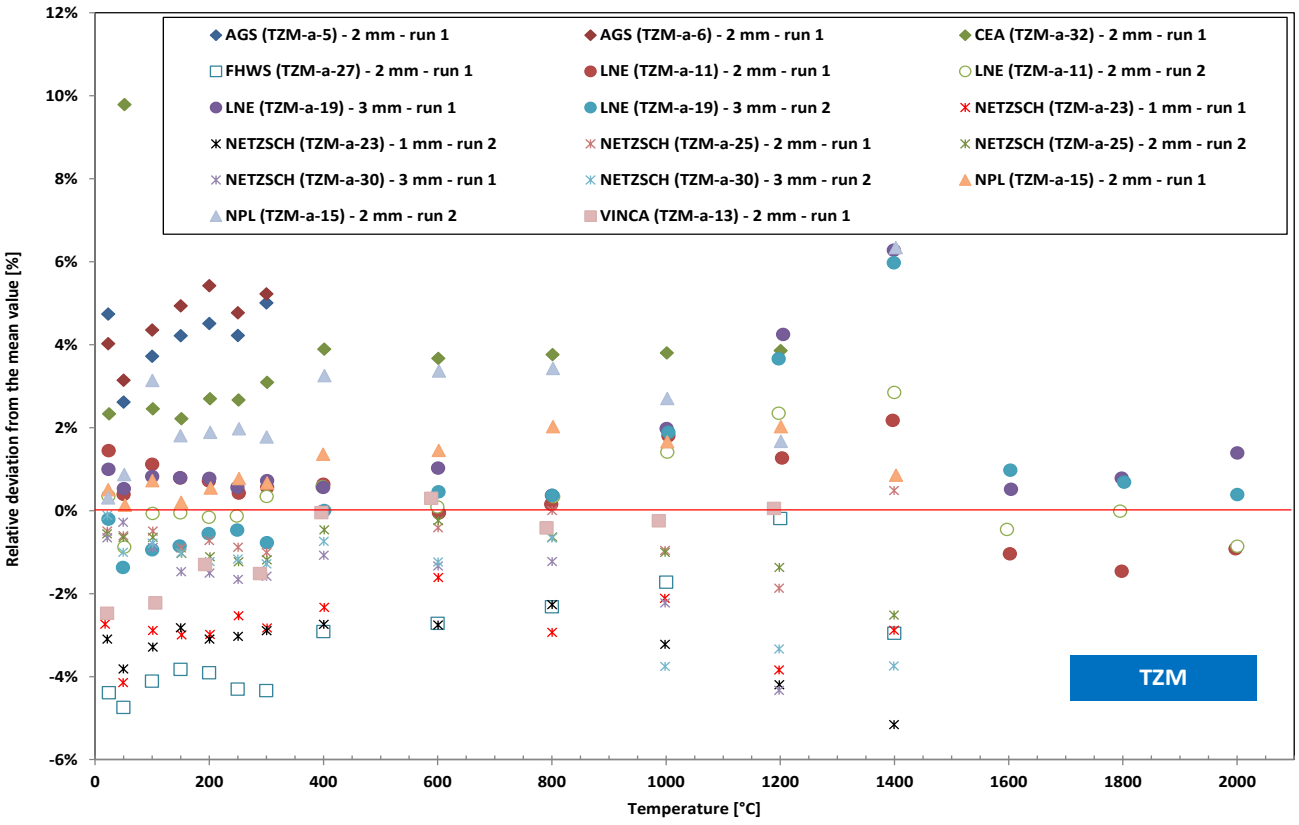

Figure 5 - TZM alloy - Relative deviation between the data obtained by the partners and the mean value determined from all results.

4.1.5 Conclusion

The metrological validation of the laser flash method for high temperature thermal diffusivity measurements has been done through the assessment of the expanded uncertainties associated to these measurements and the organization of an inter-laboratory comparison involving seven partners. The expanded uncertainties (*k=2*) associated to thermal diffusivity measurements performed by laser flash method have been estimated by the partners to be between 2.8 % to 5.0 % for temperatures higher than 1000 °C. The inter-laboratory comparison showed good agreement between results obtained by the participants from 23 °C up to the maximum temperature reached, considering the relative deviations and their uncertainties.

In order to facilitate uptake of the project results by end users, LNE, AGS, CEA, FHWS, NETZSCH, NPL and VINCA produced collectively datasets of high temperature thermal diffusivity for three refractory materials, as well as series of tutorials and a good practice guide related to these measurements.

With the reference laser flash apparatus, uncertainty budgets, datasets and documentations noted above, this objective has been fully achieved.

4.2 Objective 2: Establishing traceability for specific heat measurements at temperatures up to 3000 °C

The strategy applied to meet the needs of traceability for specific heat measurements at high temperatures has been similar to the ones used for the objectives 1 and 3, respectively focused on thermal diffusivity and spectral emissivity measurements.

Calorimeters based on different metrological approaches (drop calorimetry and pulse calorimetry) have been first developed, and the uncertainty budgets associated with the specific heat measurements were established. The performances of these facilities were compared in a second step through the specific heat measurement of three pure materials at very high temperature. They have been finally applied by the partners involved in this objective (LNE, PTB, TUG, VINCA and ZAE) to the characterisation of three typical “industrial” materials.

4.2.1 Development of a reference facilities for measuring the specific heat up to 3000 °C

Three reference facilities were developed by LNE and PTB for the measurement of the specific heat up to 3000 °C. The approach employed by LNE was to modify its LFA (described in § 4.1.1) in order to achieve measurements of specific heat based on the enthalpy increments determinations [4].

The inductive furnace of the LFA is used to heat the sample to the desired temperature of measurement. In order to be able to measure enthalpy increments, this furnace was equipped with automated pliers at its upper part and a differential heat-flux calorimeter at its bottom part to receive the heated specimen, converting the laser flash apparatus into a high temperature drop calorimeter (see Figure 6). The studied specimen is connected with a thin wire and positioned inside the heating furnace by automated pliers. The temperature of the specimen is measured using optical pyrometers covering the range from 500 °C up to 3000 °C. The pyrometers “see” the specimen using an elliptical broadband silver mirror placed at 45° on a horizontally motorised basis between the furnace and the calorimeter. Once the temperature of the specimen is measured, the mirror moves in order to let the specimen drop in the calorimeter.

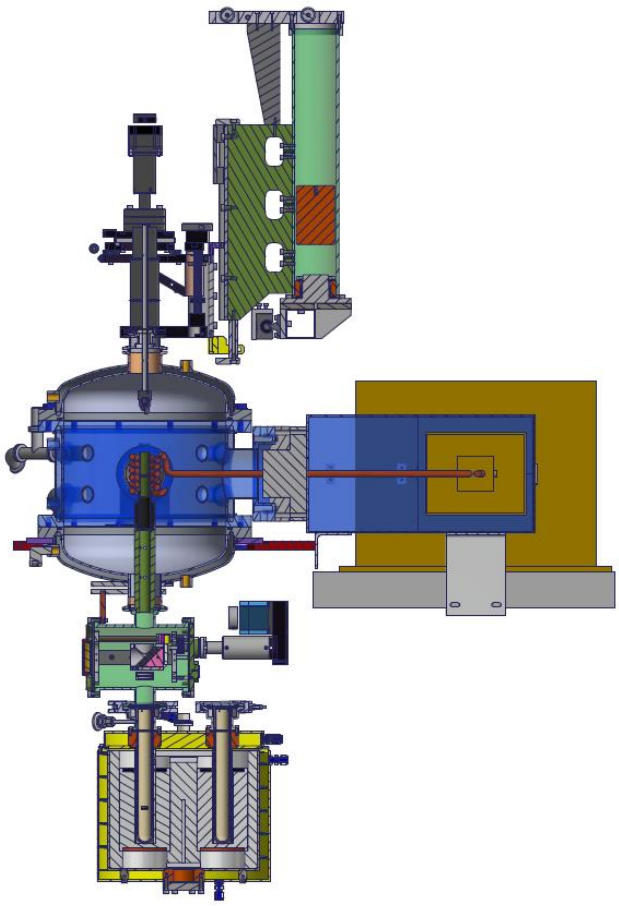

Figure 6 - Drop calorimeter developed at LNE

The used calorimeter is composed of two Calvet thermopiles plugged in an equalisation cylindrical block of aluminium. The block is maintained at near room temperature (25 °C) using temperature regulated water jacket. The two thermopiles are connected in opposition in order to compensate any temperature fluctuation of the block. The electromotive force (EMF) generated by the arrangement of the thermopiles is proportional to the difference in heat flux between the two cells. A resistance temperature detector (Pt-100) located in the calorimetric block measures the mean temperature of the measuring cells. Two identical high-density alumina tubes, closed at one end, are inserted in the calorimeter cells. The upper and open ends of the tubes are hermetically connected to the mirror box that helps in the temperature measurement of the specimen before the drop.

The specimen and its container are heated by the graphite susceptor, and its temperature is measured by a bi-colour pyrometer from Infratherm® that operates from 1000 °C to 3000 °C. The pyrometer was calibrated against a black body source, and is checked against phase transition fixed points.

At PTB the determination of the specific heat of materials by drop calorimetry is performed by using a copper block type calorimeter in isoperibol operating mode. The isoperibol operating is characterized by an isothermal surrounding while the temperature of the calorimeter system changes during a measurement. As a result, a temperature exchange occurs between the system under investigation and the isothermal surrounding. A cylindrical shape of the copper block allows an almost homogenous temperature distribution. Thus a precise measurement of the enthalpy rise can be performed.

The specimen is heated by an induction furnace and is held in position by a thin tungsten wire which is fastened to a supply roll. An optical pyrometer measures the temperature of the specimen in the range of 700 °C up to 3000 °C. When the specimen reaches the desired temperature it is lowered by a stepper motor into a tungsten crucible inside of the copper block. Due to the high temperatures that will be reached during the measurement series and in order to reduce heat loss during the heating period, the whole calorimeter systems is evacuated up to a pressure of 5.4×10^{-4} hPa with a vacuum facility.

The second approach by PTB for measuring the specific heat is a further development of the dynamic emissivity measurement [5]. Both measurements are based on a modified laser-flash apparatus (Figure 7), which is commonly used to determine the thermal diffusivity. The dynamic emissivity measurement was adapted to use its principle to determine the specific heat, if the emissivity of the sample is known.

The sample under investigation is heated to the desired temperature (T > 750 °C) via inductive heating. When a temperature equilibrium is reached, the front side of the sample is heated by a short, high-energy laser pulse of energy E. This results in a temperature rise of the backside of the sample ΔT of a few Kelvin. This characteristic temperature rise is recorded by an absolutely calibrated radiation thermometer. If the emissivity and mass m of the sample are known the definition of the heat capacity can be used to determine the specific heat.

It is assumed that the spectral absorption is equal to the spectral emissivity at the same wavelength as governed by Kirchhoff's law. Therefore the radiation thermometer has the same central wavelength of λ = 1064 nm as the laser. The adiabatic temperature rise ΔT_{adi} of the sample can be described by solving the heat transfer equations for certain boundary conditions. The measured temperature rise can be fitted by a mathematical model that accounts for heat losses via radiation and convection among other things.

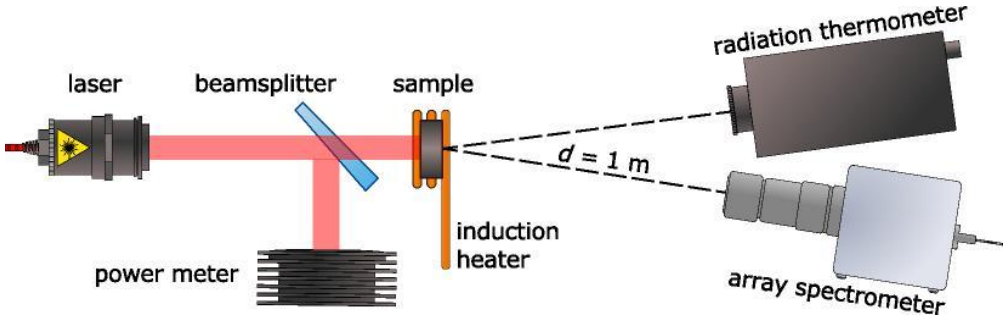

Figure 7 - Laser-flash based calorimeter developed by PTB

4.2.2 Assessment of uncertainty on very high temperature specific heat measurements

Tungsten, molybdenum and isotropic graphite were chosen as potential reference materials and an inter-laboratory comparison was performed. Based on the test results the uncertainty budget of the different measuring methods was estimated by LNE, PTB, TUG, VINCA and ZAE. All the results from the inter-laboratory tests are compiled in **Error! Reference source not found.**, Figure 9 and Figure 10. The isotropic graphite sample could not be measured by all the partners as the material is not suitable for all the used measuring methods, which are listed in Table 3.

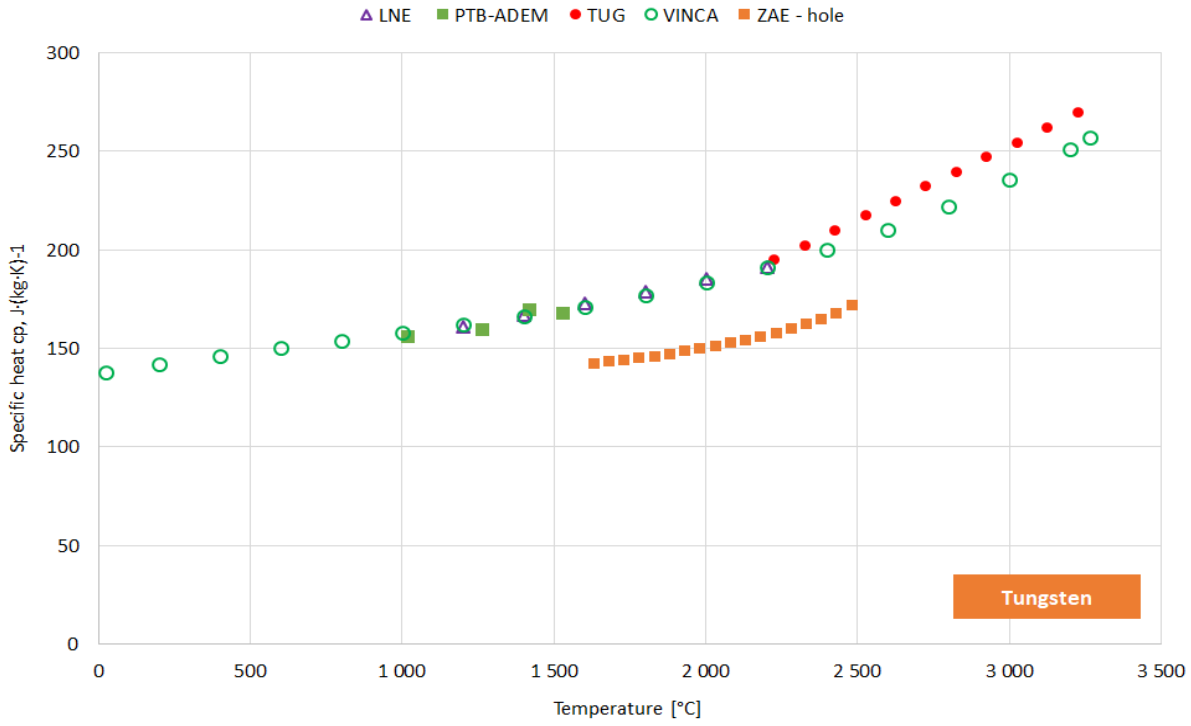

Figure 8 - Specific heat values measured on tungsten

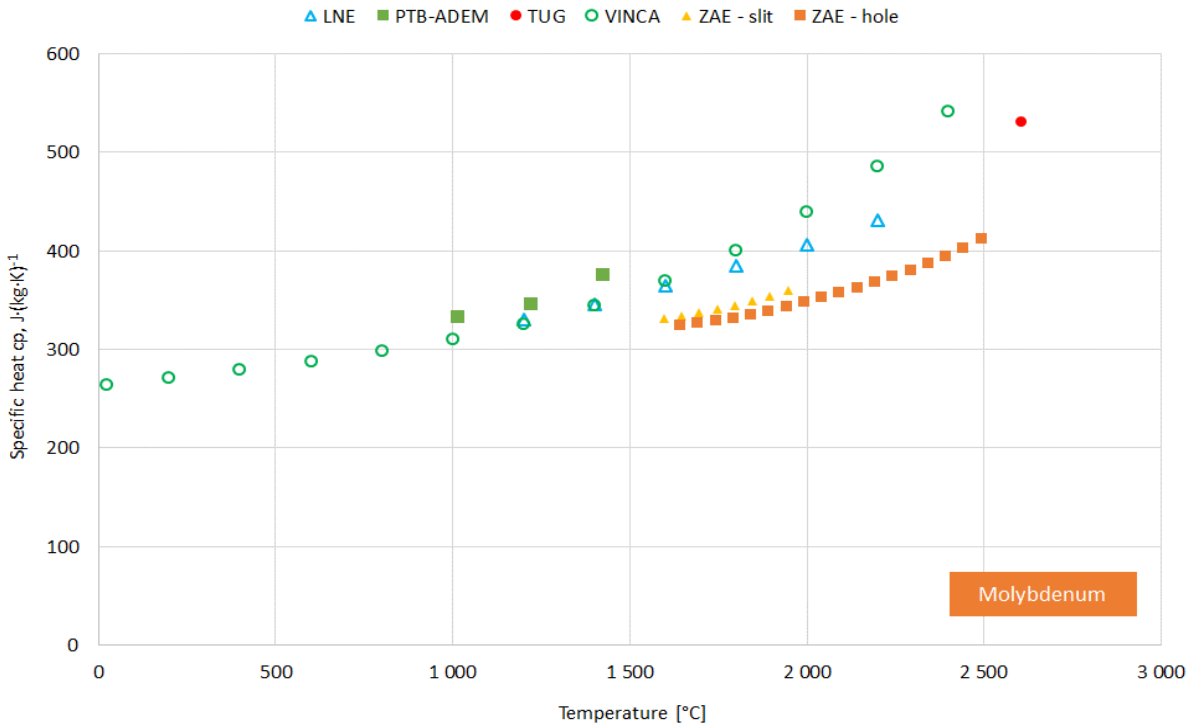

Figure 9 - Specific heat values measured on molybdenum

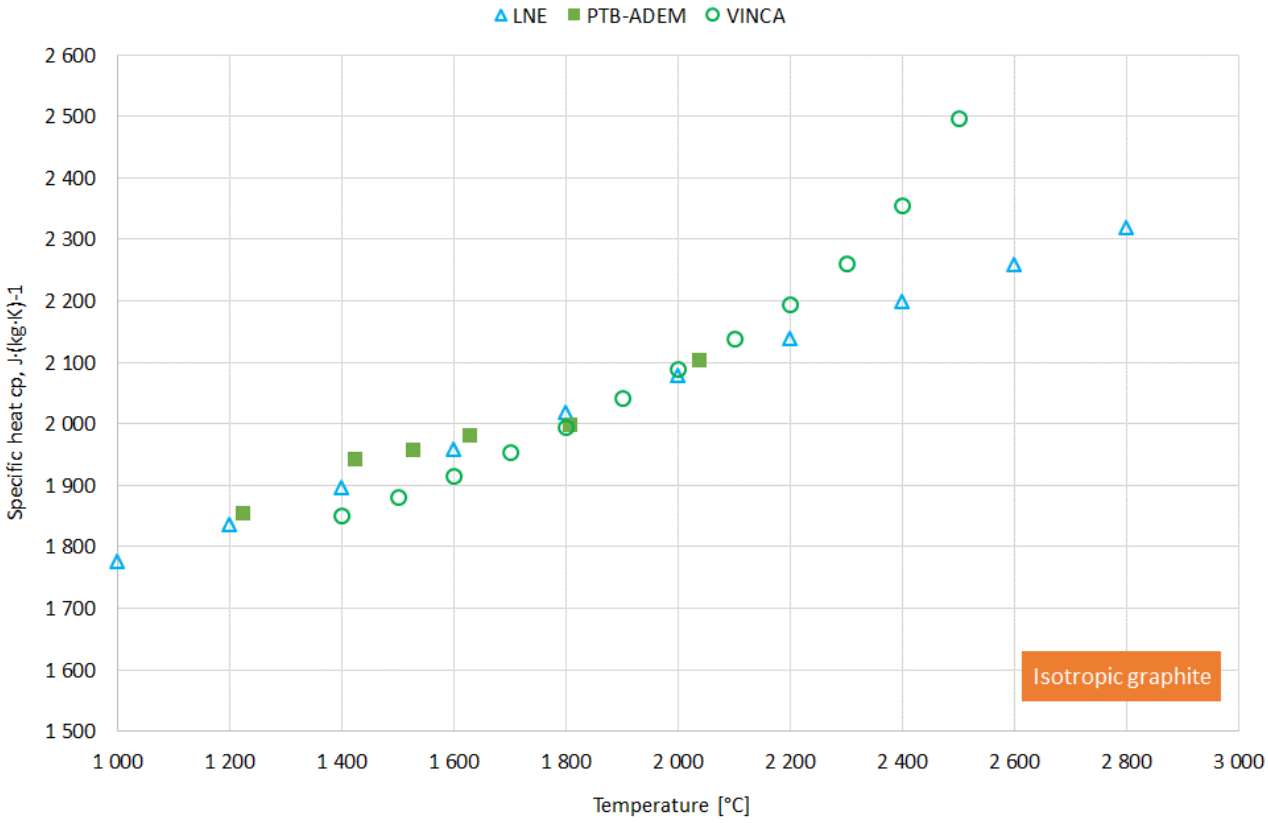

Figure 10 - Specific heat values measured on isotropic graphite

The expanded uncertainty (*k=2*) estimated for the specific heat measurements of tungsten, molybdenum and isotropic graphite are given in Table 3 for all the partners and measuring methods.

Table 3 Expanded relative uncertainties (*k=2*) for the measurements on reference materials

Partner	Apparatus	Material	Expanded relative uncertainty (*k*=2)
LNE	Drop calorimeter	Tungsten Molybdenum Isotropic graphite	3.5 %
TUG	Pulse heating calorimeter	Tungsten Molybdenum	8.0 %
ZAE	Pulse heating calorimeter	Tungsten Molybdenum	21.5 %
VINČA	Pulse heating calorimeter [6]	Tungsten Molybdenum Isotropic graphite	7.0 % 11.0 % More studies needed
PTB	Flash based calorimetry	Tungsten Molybdenum Isotropic graphite	12 % 12 % 9 % < u_{rel} < 16 %

4.2.3 Specific heat measurements on industrial materials

Measurements were performed by LNE, VINCA and PTB by using the facilities developed in this project on the following industrial materials: TZM (a molybdenum alloy), C/SiC and SiC/SiC composite materials.

An example of specific heat values obtained at very high temperature with the TZM alloy is shown in Figure 11 with uncertainty bars evaluated by the partners. A good agreement within 10 % between values measured by LNE, VINCA and PTB can be observed up to 2000 °C. Larger deviations were observed for the measurements performed on the C/SiC and SiC/SiC samples.

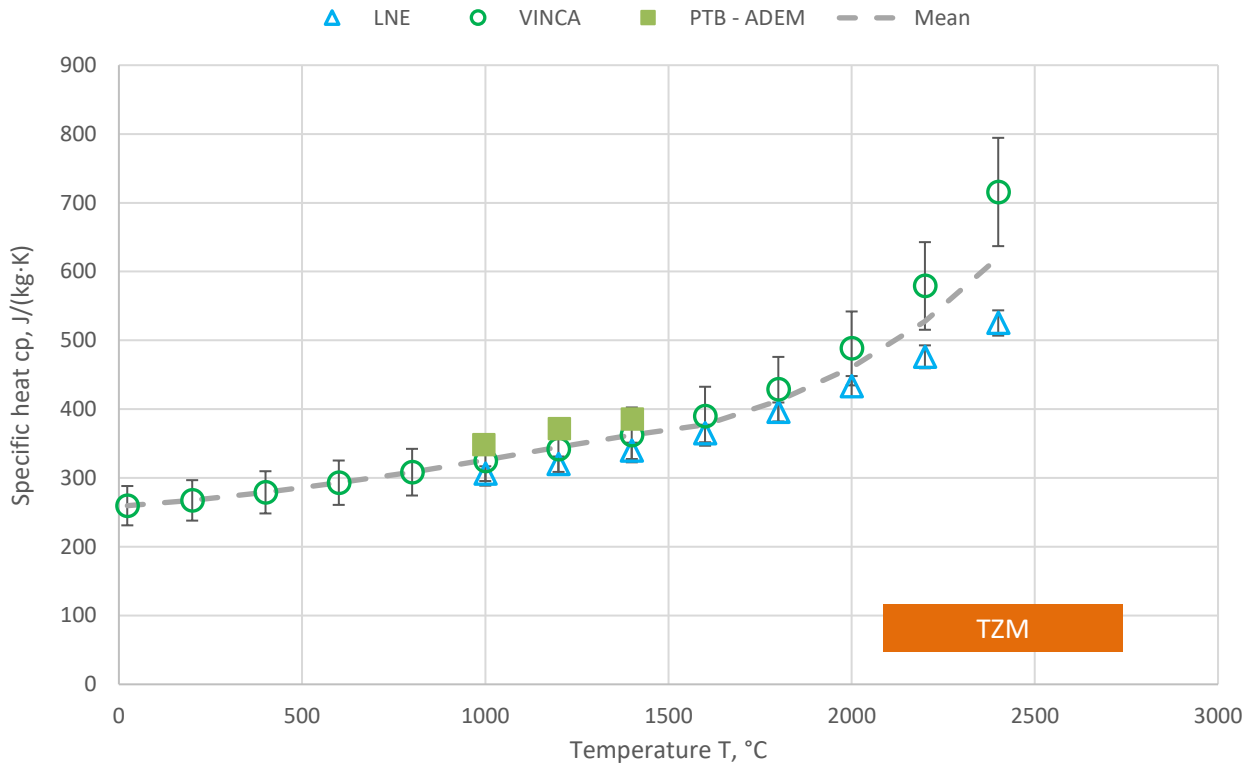

Figure 11 - Specific heat values measured on TZM

4.2.4 Conclusion

The objective 2 was successfully achieved with the development of three reference facilities for the traceable measurements of specific heat up to 3000 °C. These calorimeters were applied to the characterisation of the specific heat of different refractory materials in a large temperature range.

The uncertainties associated with high temperature specific heat measurements have been assessed for the two metrological approaches used (pulse-heating or drop calorimetry).

The collaboration between LNE, PTB, TUG, VINCA and ZAE produced datasets of high temperature specific heat for tungsten, molybdenum and isotropic graphite. This collaboration also enabled to demonstrate that the original uncertainty target of 1.5 % above 1000 °C was not achievable due to technical difficulties and changes or contaminations of the specimens, and that an expanded uncertainty (k=2) of about 5 % to 10 % was a more realistic value at the highest temperatures.

4.3 Objective 3: Establishing traceability for emissivity measurements and improved metrology for temperature of fusion at temperatures up to 3000 °C

Spectral emissivity at high temperatures is a crucial thermophysical (surface) property for temperature measurements via radiation thermometry, heat transfer calculations and thermal modelling. The temperature range above 1000 °C is experimentally difficult to access for a reproducible emissivity determination as the sample surface is easily altered due to chemical reactions with its environment. One approach to overcome this dilemma is to heat up and measure the sample quickly before alterations of the sample surface become prominent (e.g. the ohmic pulse-heating apparatus (OPA) at TUG reaches a temperature of 3000 °C within a few ten microseconds). Input parameter for thermal modelling the knowledge of spectral emissivity is desired over a broad spectral range. For this reason, the EMMA facility at ZAE was designed to determine the spectral emissivity in a spectral range between 1 □m and 20 □m. This objective aimed to develop a strategy to assess existing and newly developed or improved setups for the measurement of spectral emissivity. This cannot be achieved over the full range experimental capabilities (with regard to temperature or spectral range, sample size or sample type) but instead only for the overlapping measurement regions.

4.3.1 Development of a reference facility for measuring the spectral emissivity

At PTB, a dynamic method for measuring the spectral emissivity at temperatures above 1500 K was improved significantly towards higher temperatures within the frame of the Hi-Trace project. The measurement scheme is based on a modified commercial laser-flash apparatus (cf. Figure 7, the same facility being used in Objective 2 to determine the specific heat when spectral emissivity is known).

In this device the sample with known mass and heat capacity is heated in a furnace and once the sample has reached a temperature equilibrium (e.g. at 2000 °C) a short, high-energy laser pulse (ND:YaG laser with pulse length of around 1 ms and energy of roughly 1 J) is used to further heat the sample. The resulting temperature rise of around 1 K to 3 K is measured with a radiation thermometer. By using a well characterized optical beamsplitter a defined, reflected portion of each laser pulse is measured in situ by a power meter and the laser energy hitting the sample can be determined. The emissivity at 1064 nm can be derived from the characteristic temperature rise measured by the high-speed radiation thermometer. The spectral radiance is measured by the array-spectrometer while the sample is temperature stabilized to determine the emissivity in a spectral range from 550 nm to 1100 nm. The setup was improved by introducing a well characterized array-spectrometer to extend the spectral emissivity measurement to a range from 550 nm to 1100 nm, by changing to inductive heating (max. power of p = 6 kW and f = 240 kHz) to reduce effects of interreflection between the furnace walls and the sample and by dedicated high-temperature sample holders optimized for inductive heating.

The direct measurands are only the laser energy hitting the sample and the adiabatic temperature rise of the sample. Central wavelength, transmissivity of the output window and mass of the sample are separately measured and only parameters in the measurement equations. For determining the spectral emissivity, the specific heat is needed from external measurements or literature data. For the measurement results here data for the specific heat determined in Objective 2 were used.

A Monte Carlo method has been developed to calculate the uncertainties regarding the dynamic emissivity measurement according to the modified GUM S1 adaptive scheme.

4.3.2 Emissivity Measurement Apparatus (EMMA) at ZAE

At ZAE the emissivity measurement apparatus (EMMA) has been developed especially for determining the emissivity of opaque specimens with vanishing transmissivity at high temperatures. In this set-up an FTIR-spectrometer is used to compare the radiation of the sample to the radiation of a blackbody radiator (both at the same temperature).

The measurement apparatus has been built up with novel customized components, providing an enhanced performance, especially higher accessible temperatures due to an inductive heating unit. Additionally, a new vacuum vessel and an optimized beam path with movable mirrors have been installed. A detailed description of the improved EMMA can be found in [7], a sketch is depicted in Figure 12.

Depending on the material of the specimen, the specimen can then be heated either directly by induction or indirectly from the backside, where the hot graphite cylinder is located. The radiation coming from the blackbody or the specimen, respectively, is guided by different mirrors to the FTIR-spectrometer and is finally detected by the integrated IR-detector. For this purpose, the vacuum vessel is coupled to a Bruker FTIR-spectrometer Vertex 70v.

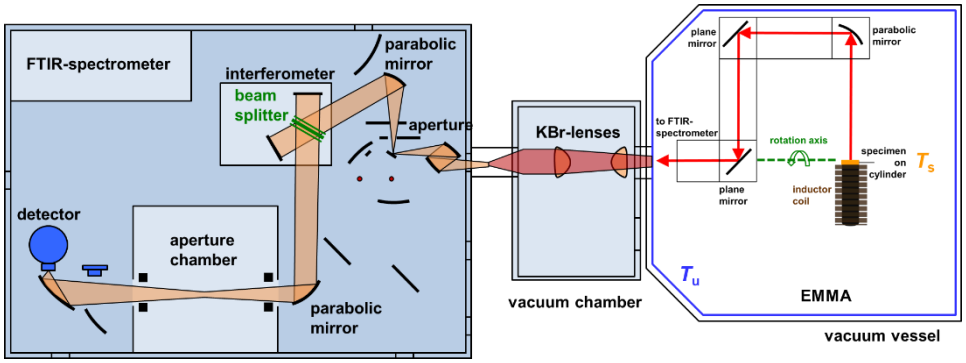

Figure 12- Sketch of the improved EMMA. The inductor is placed in the vacuum vessel on the right, which is coupled to the FTIR-spectrometer Vertex 70v on the left by an additional vacuum chamber in the middle. The intensity emitted by the specimen is detected by the spectrometer. The whole beam path can be evacuated.

4.3.3 Ohmic pulse-heating apparatus with a µs-DOAP at TUG

At TU Graz (TUG) the normal spectral emissivity of solid and liquid is measured by a combination of an ohmic pulse-heating apparatus with a µs-DOAP. Here, a large current pulse (some 1000 A) is distributed through a wire-shaped sample, with a diameter of 0.5 nm. Due to its electrical resistivity, the sample heats up, melts, and it reaches the material's boiling point. The whole process of heating up through the solid phase, melting, and passing through the liquid phase only takes around 30 µs to 50 µs. Besides the prevention of chemical reactions with any surroundings, this short experimental time also ensures that the liquid wire can be observed, without collapsing due to gravitational forces. The spectral emissivity is simultaneously determined by a fast Microsecond Division of Amplitude Photopolarimeter (□s-DOAP).

4.3.4 Inter-laboratory comparison on spectral emissivity measurements

These facilities were used in an inter-laboratory comparison on spectral emissivity measurements in order to validate the different approaches applied and to estimate the associated uncertainties using the experimental results. Samples of molybdenum, tungsten and graphite were identified as suitable materials for this inter-laboratory comparison. Mo and W samples were sandblasted in order to improve sample to sample uniformity.

In test measurements at ZAE and PTB the emissivity was observed to change during the initial heating, this annealing effect appeared to stabilize after the samples were exposed to a maximum temperature. For this reason, the partners agreed to initially heat the samples to a temperature 50 K above the highest measurement temperature in order to anneal the surface properties of the sample. ZAE and PTB also investigated the change in surface structure using EDX and electron microscopy, it was observed that upon heating potential contamination on the surface is removed and the fine surface structure of the sample smoothens.

The required sample geometry is different for each participant, while for PTB and ZAE samples were of cylindrical shape (but different sizes), the samples for TUG are in the form thin wires and due to this special geometry samples could not be prepared for graphite.

Out of the measured data by each participant those wavelength and temperature intervals (e.g. wavelength interval 600 nm to 2 □m) were selected which allow a direct comparison with between the partners. ZAE provided measurement data over a broader measurement range (1 □m – 20 □m), TUG was able to investigate the spectral emissivity at 685 nm in the solid and liquid phase and up to 4000 K.

The achieved measurement uncertainties are stated below for all measured temperatures. Diagrams are presented exemplarily to illustrate the agreement between the different measurement techniques for graphite (Figure 13), tungsten (Figure 14**Figure 13** and Figure 15) and molybdenum (Figure 16 and Figure 17).

For Graphite the achieved uncertainties (all *k*=1) at PTB were between 2.6 % for 1473 K, 3.0 % for 1673 K, 5.1 % for 2073 K for a wavelength of 1064 nm and for the spectral range between □□= 500 nm and 1100 nm average uncertainties of 7.3 % at a temperature of 1473 K, 7.8 % at 1673 K and 11 % at a temperature 2073 K were observed for the spectrally resolved emissivity which utilized an array spectrometer. At ZAE the achieved measurement uncertainties were between *u* (1 □m) = 4.9 %, *u* (10 □m) = 0.9 % and *u* (20 □m) = 0.9 % for a temperature of 1473 K; *u* (1 □m) = 4.3 %, *u* (10 □m) = 0.8 % and *u* (20 □m) = 0.9 % for a temperature of 1673 K and *u* (1 □m) = 3.5 %, *u* (10 □m) = 0.8 % and *u* (20 □m) = 0.9 % for a temperature of 2073 K.

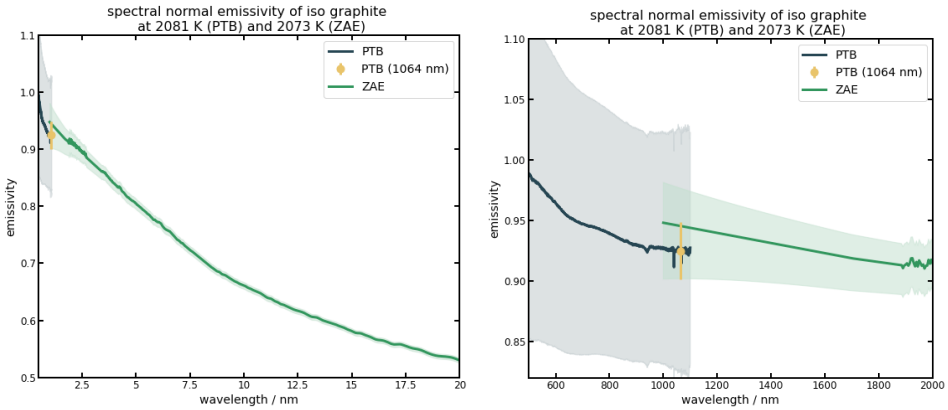

Figure 13 - Normal spectral emissivity of graphite at 2073 K in the spectral range between 0.55□□m and 20 □m (left) and between 0.55□□m and 2 □m (right)

For tungsten samples the achieved uncertainties (all *k*=1) are between 3.7 % for 1473 K, 4.3 % for 2000 K , 5 % for 2384 K for PTB measurements at a wavelength of 1064 nm. For the spectral range between □□= 500 nm and 1100 nm average uncertainties for the spectrally resolved emissivity measurements which utilized an array spectrometer of 9.0 % at a temperature of 1473 K, 8.6 % at 2000 K and 11.2 % at a temperature 2384 K were observed at PTB. At ZAE the achieved measurement uncertainties for the spectral emissivity were between *u* (1 □m) = 10.5 %, *u* (10 □m) = 1.7 % and *u* (20 □m) = 1.6 % for a temperature of 1473 K, *u* (1 □m) = 7.5 %, *u* (10 □m) = 1.5 % and *u* (20 □m) = 1.4 % for a temperature of 1923 K and *u* (1 □m) = 6.1 %, *u* (10 □m) = 1.4 % and *u* (20 □m) = 1.3 % for a temperature of 2373 K. At TUG the spectral emissivity was measured in the temperature range between 2000 K and 4000 K at a wavelength of 684.5 nm. The measurement uncertainty was in the order of 10 % for the solid state and around 30 % for the liquid state for temperatures above 3500 K.

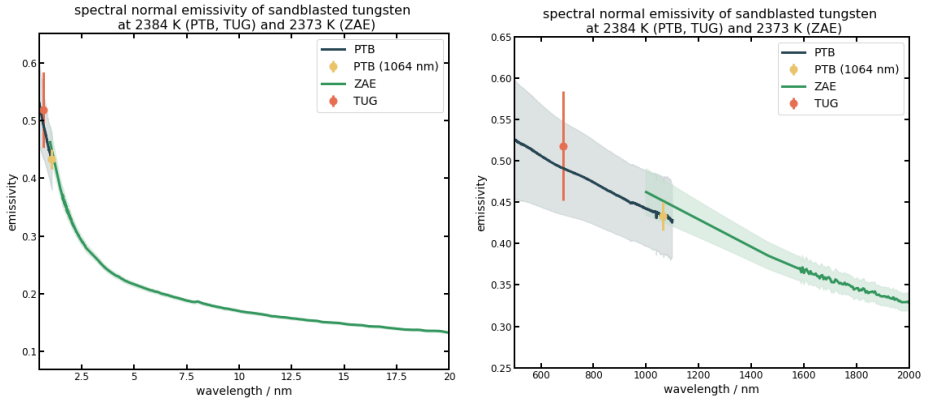

Figure 14 - Normal spectral emissivity of tungsten at 2384 K in the spectral range between 0.55□□m and 20 □m (left) and between 0.55□□m and 2 □m (right)

For molybdenum samples the achieved uncertainties (all *k*=1) for PTB were between 3.8 % for 1250 K, 4.3 % for 1843 K, 4.1 % for 2032 K for PTB at a wavelength of 1064 nm. For the spectral range between □□= 500 nm and 1100 nm average uncertainties for the spectrally resolved emissivity measurements which utilized an array spectrometer of *u* = 9.2 % at a temperature of 1373 K, *u* = 10.1 % at 2000 K and *u* = 9.5 % at a temperature 2030 K were observed. At ZAE the achieved measurement uncertainties for the spectral emissivity were between *u* (1 □m) = 10.5 %, *u* (10 □m) = 1.7 % and *u* (20 □m) = 1.6 % for a temperature of 1373 K, *u* (1 □m) = 7.9 %, *u* (10 □m) = 1.5 % and *u* (20 □m) = 1.4 % for a temperature of 1823 K and *u* (1 □m) = 7.0 %, *u* (10 □m) = 1.5 % and *u* (20 □m) = 1.4 % for a temperature of 2073 K. At TUG the spectral emissivity of molybdenum was measured in the temperature range between 1700 K and 3200 K at a wavelength of 684.5 nm.

The measurement uncertainty was in the order of 20 % for the solid state and around 10 % for the liquid state for temperatures above 2600 K.

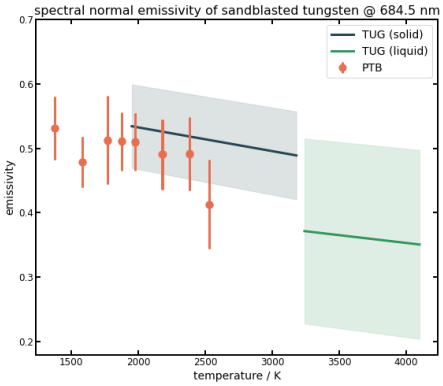

Figure 15 - Normal spectral emissivity of tungsten (solid and liquid) at a wavelength of 684.5 nm and over a temperature range between 1300 K and 4000 K

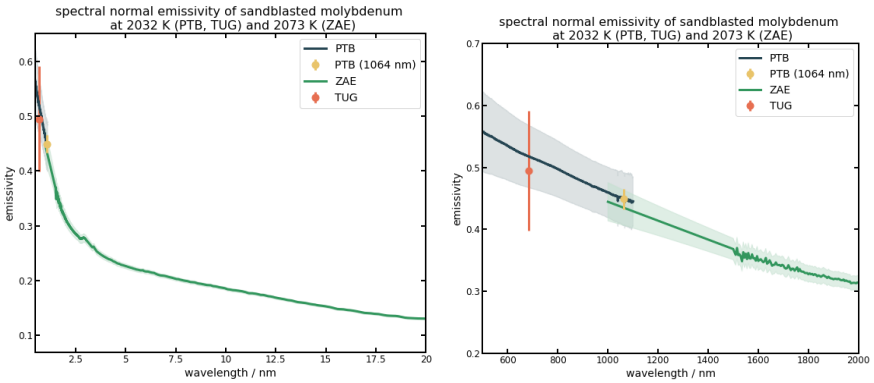

Figure 16 - Normal spectral emissivity of molybdenum at 2032 K in the spectral range between 0.55□□m and 20 □m (right) and between 0.55□□m and 2 □m (left)

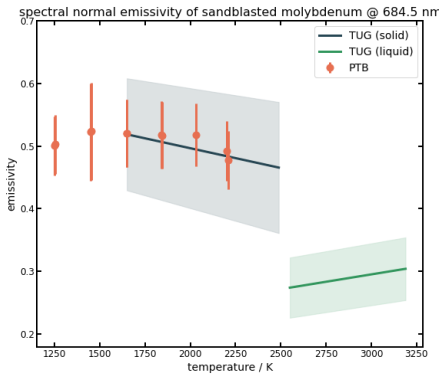

Figure 17 - Normal spectral emissivity of molybdenum (solid and liquid) at a wavelength of 684.5 nm and over a temperature range between 1250 K and 3200 K

4.3.5 Metrology for temperature of fusion

There are more than 300 known materials with a melting temperature exceeding 2000 °C. About fifteen of them melt at a temperature higher than 3000 °C. They find use or are candidates for many applications, including aerospace and power plants. The best choice for each application is based on several engineering criteria. The melting temperature, however, marks the absolute limit up to which a (solid) material can serve its function. Its accurate measurement is, therefore, important. In order to avoid many of the challenges presented by high-temperature measurements and to limit some of the issues related particularly to the containment of a molten sample, it is generally preferable to limit as much as possible the measurement time. This has been the driving force for the development of measurement techniques based on rapid heating, such as pulse-heating or inductive heating.

The following paragraphs present the facilities developed or improved by three partners (JRC, TUG, ZAE) during the project for measuring temperature of fusion up to 3000 °C. Their techniques differ and are characterised by distinct strengths and limitations. Broadly speaking, they can be classified into surface heating (JRC) and volume heating techniques (TUG, ZAE).

Laser-heating setup at JRC

Two laser-heating systems are used at JRC for the measurement of melting temperatures. The first one is applied to non-radioactive specimens and those containing uranium as the only radioactive element. It is an easily accessible setup on an optical table with quick turnaround times. The second one can be used for more radioactive specimens, such as mixed uranium-plutonium oxides. Therefore, a glovebox is needed to contain the radioactive material and shield the operators from α-radiation (cf. Figure 18). The two systems are identical in principle and differ in practice only with respect to a few ancillary components, e.g. the type of vacuum pump and the control of the buffer gas.

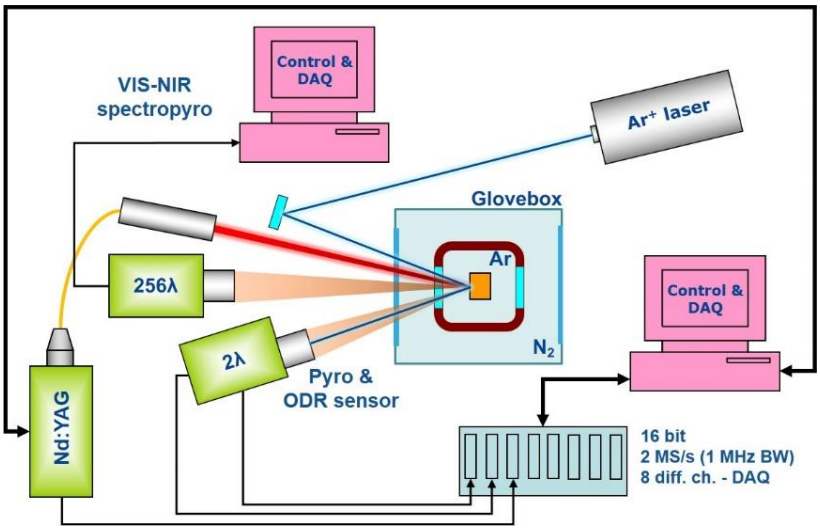

Figure 18 - Schematic of the glovebox setup at JRC

In a typical experiment, the specimen is heated through the melting transition by a powerful laser and then allowed to cool down naturally. Plateaus and inflections in the recorded thermogram, i.e. the temperature-vs-time trace, reveal phase transitions, including melting and solidification. By focusing the laser onto a small spot, quasi-containerless conditions are established, in which the colder periphery and deeper layers of the specimen act as a crucible for the volume of interest, thus preventing interaction and contamination with foreign material from the specimen holder. Furthermore, due to the short penetration depth of laser light into an absorbing material, the amount of matter being heating to the highest temperature is relatively small and, thus, extremely high surface temperatures can be attained in short times.

Both electrically conducting and insulating materials can be investigated as long as they sufficiently absorb light at the laser wavelength. Specimens can be of irregular shape although typically they are cylindrical or rectangular, with lateral dimensions of a few millimetres and a thickness ranging from sub-millimetre to more than 10 mm. In order to minimise the conductive heat losses, they are held in three- of four-pin mounts (cf. Figure 19).

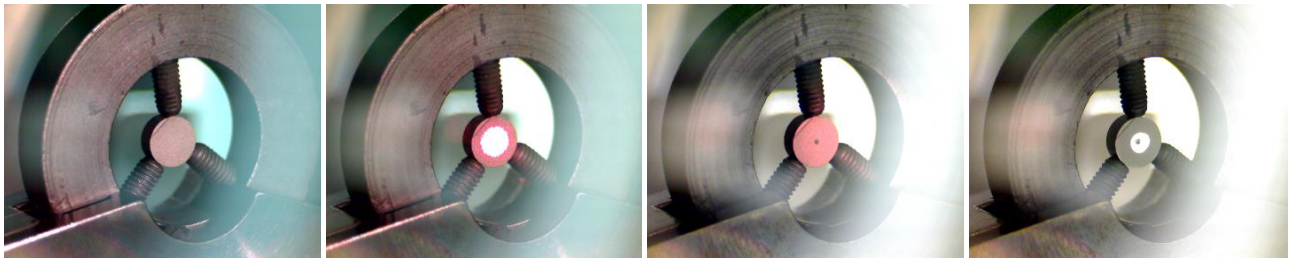

Figure 19 - A mounted tungsten specimen. From left to right: before the experiment, with the visible pilot laser on for alignment purposes, with the pyrometer measurement spot projected onto it, and after the first melting experiment. The shiny area indicates the molten and re-solidified region.

Several high-speed radiation thermometers, commonly known as pyrometers, are available for the measurement of radiance temperature. They operate in the visible and near-infrared spectral region. The main pyrometer used in Hi-TRACE operates near 650 nm with a FWHM bandwidth of 27 nm. Logarithmic amplification of the photocurrent generated by a Si PIN photodiode allows the coverage of a very wide temperature range. A holographic notch filter mounted in front of the pyrometer lens largely rejects parasitic Nd:YAG laser light reflected off the specimen. The pyrometer was calibrated using PTB-calibrated tungsten ribbon lamps up to a radiance temperature of 2500 K.

A 256-channel Si photodiode-array (PDA) spectrometer is simultaneously used to acquire radiance spectra during the experiments. In the temperature range of interest for Hi-TRACE, integration times of 4 s and 8 ms were used resulting in a total data acquisition time of 1 s or 2 s, respectively. The spectrometer was calibrated against a gas-filled tungsten ribbon lamp with a PTB-issued calibration certificate for spectral radiance in the wavelength range of 0.5 µm to 2.5 µm at a radiance temperature near 2500 K at 650 nm.

An Ar^+ laser with an optical power of 0.75 W at 488 nm is used as a probe laser to facilitate the detection of phase transitions and, particularly melting and solidification. This blue probe laser illuminates the specimen in a concentric fashion with the Nd:YAG laser spot and the pyrometer spot. The pyrometer is equipped with a narrow-bandwidth channel centred at the same wavelength to detect blue laser light reflected off the specimen. The technique is based on the fact that phase transformations are often accompanied by changes in reflectance.

Ohmic pulse-heating apparatus (OPA) at TUG

An ohmic volume-heating technique is applied at TUG to heat specimens through the melting transition into the liquid region and all the way to boiling and the resulting phase explosion in a matter of tens of microseconds. This way, the wire-shaped specimens retain their shape in the liquid region allowing thermophysical properties of molten refractory materials to be measured in this otherwise inaccessible regime. Another advantage of the technique is its quasi-containerless nature, as the molten specimens do not need to be contained by a crucible but, instead, are held in place by inertia during the short experiment duration. The technique is limited to electrically conducting materials that can be produced in the required shape.

The specimens are self-heated by an electric current of several kiloamperes that is driven through them. A large capacitor bank of 500 µF is used to store the energy before the electric pulse is released. Ultra-fast ignitrons are then used to switch the large current.

The temperature is measured in a non-contact manner by a radiation thermometer operating at a wavelength of 650 nm. The measurement of the electric current through the specimen with a Pearson probe, the voltage drop across the specimen with suitable Mo electrodes in contact with the specimen, and the radial thermal expansion of the specimen with a microsecond-resolution CCD camera allow the determination of several important thermophysical properties in the solid and liquid phase. The system is completed by a microsecond-resolution division-of-amplitude-photopolarimeter (DOAP) for the measurement of the optical constants of the specimen at 684.5 nm, from which the normal spectral emittance is computed.

The DOAP consists of a diode laser at 684.5 nm, a polarisation state generator (PSG), and a polarisation state detector (PSD). The PSG produces a defined state of polarisation of the laser light that is incident on the specimen with an angle of incidence of 70°. The polarisation state detector then analyses the polarisation state of the reflected laser light and determines the optical constants from the change of polarisation upon reflection by the specimen. The measurement assumes reflection off ideally smooth surfaces, but seems to be resilient to some small degree to surface roughness in the solid state.

Emissivity measurement apparatus (EMMA) at ZAE Bayern

While EMMA has been developed and further improved during Hi-TRACE specifically for the measurement of directional spectral emittance over a wide wavelength and temperature range (cf. § 4.3.2), it can also be used to measure the melting temperature of a specimen. This is thanks to the new inductive heating unit that has 5 kW of power available to melt even refractory materials at a fast heating rate (cf. Figure 20). Containment of the molten specimen, however, poses a challenge and will benefit from further development. The significant advantage of this system, compared to the systems at JRC and TUG, is that it provides a direct measurement of the directional spectral emittance of the specimen, regardless of its surface state, which is required to convert the radiance temperature measured by a radiation thermometer to true temperature.

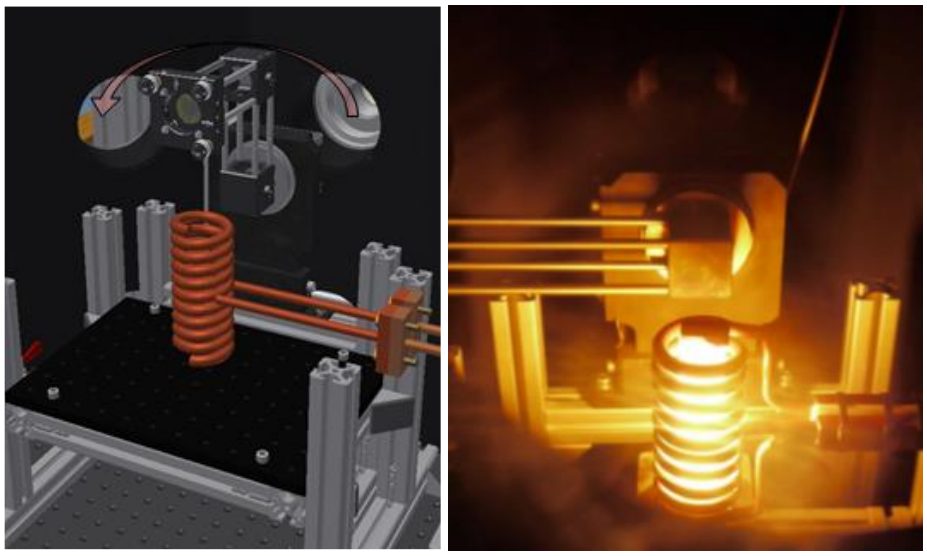

Figure 20 - Schematic of the setup of the inductor inside the vacuum vessel with movable mirror arm on the left and photo of inductor with heated reference blackbody on the right.

4.3.6 Conclusion

A reference facility for the traceable measurement of spectral normal emissivity of solid materials was established at PTB. Samples of graphite, tungsten and molybdenum were investigated at PTB and ZAE with respect to the effect of sandblasting and heat treatment on uniform surface roughness and reproducible measurement results for spectral emissivity. As a result, sandblasted samples (for W and Mo) and a defined heating procedure were developed for the comparison of spectral emissivity measurements between PTB, ZAE and TUG. These three partners measured the spectral emissivity of the prepared samples in a temperature range between 1400 K and up to 4000 K and over a broad spectral range between 0.65 µm and 20 µm.

PTB, TUG and ZAE developed and analysed their measurement uncertainties. The uncertainties vary with temperature, wavelength and from sample to sample. For certain combinations of temperature and wavelength the uncertainty target of 3 % is met both at PTB and ZAE. For all three materials the observed spectral emissivities agreed within the measurement uncertainties for overlapping temperature and spectral ranges.

Facilities were also improved by JRC, TUG and ZAE for the measurements of temperature of fusion of materials at temperatures between 1500 °C and 3000 °C. These facilities were used to measure the temperature of fusion of specimens of tungsten and molybdenum

With the facilities, uncertainty budgets and datasets of spectral emissivity produced jointly by PTB, TUG and ZAE, this objective has been successfully achieved.

4.4 Objective 4: Establishing methods for quantifying de-bonding at high temperature (above 1000 °C)

De-bonding phenomena of thermal barrier coatings applied onto turbine blades have been studied before. The existing approaches for non-contact and non-destructive techniques for quantifying the state of adhesion of such coatings by using optical or infrared radiation were not satisfactory and not validated. The present project has gone beyond the state-of-art by providing validated measurement facilities of thermal contact resistance, dedicated reference artefacts and numerical tools that have been used for characterising the state of de-bonding at temperatures from room temperature to above 1000 °C.

4.4.1 Development of measurement methods

a) Development of laser-flash based method for determining thermal contact resistance at FHWS

At FHWS a commercial laser-flash-apparatus manufactured by Netzsch has been extended. In addition to the usual measurement of the sample´s backside temperature, the modified LFA allows the simultaneous measurement of the sample´s front side temperature. The principle is shown in Figure 21.

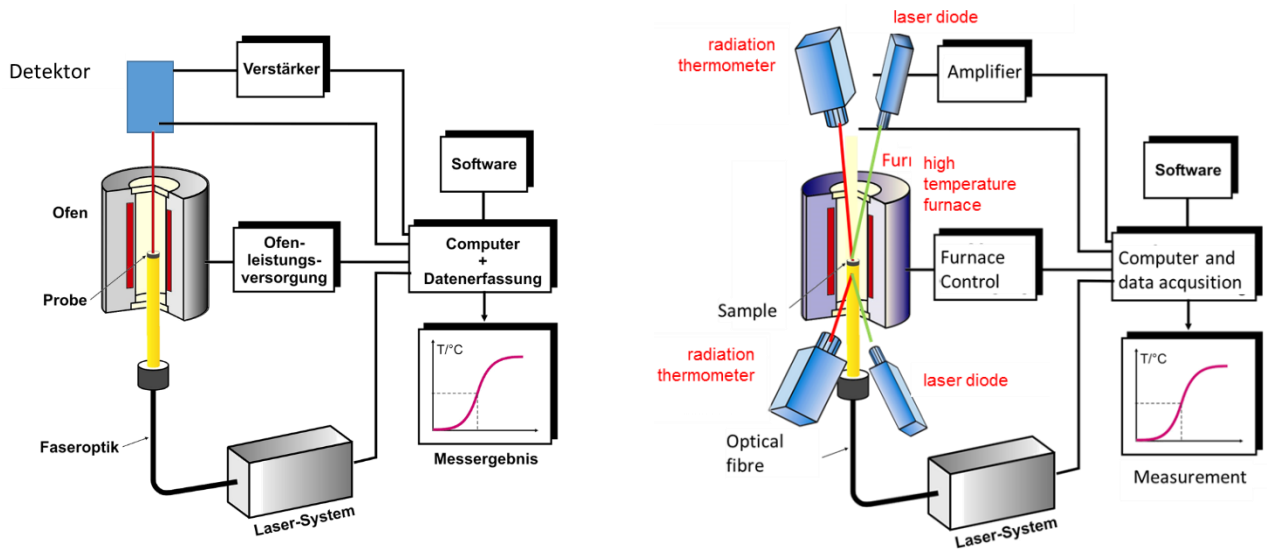

Figure 21 - Scheme of the laser flash modification. Left side: standard setup, right side: modified setup

b) Development of spectroscopic methods for emittance and thermal imaging measurements at ZAE

At ambient temperature a FTIR-spectrometer with an integrating sphere setup at ZAE Bayern has been used for measuring the spectral directional-hemispherical reflectance $R_{dh,\square}$ and transmittance $T_{dh,\square}$ of alumina (Al_2O_3) and partially yttria (Y_2O_3) stabilized zirconia (ZrO_2), which is usually abbreviated as PYSZ. For determining the infrared-optical properties at high temperatures, the black-body boundary conditions (BBC) method has been improved. With the BBC the spectral directional emittance $\varepsilon_{d,\square}$ and the spectral directional hemispherical transmittance $T_{dh,\square}$ can be measured at high temperatures as well as the spectral directional hemispherical reflectance $R_{dh,\square}$.

Finally, an experimental arrangement has been developed at ZAE Bayern in order to perform measurements of the thermal contact resistance at different wavelengths. For performing the measurements, a sapphire sample has been placed directly onto a substrate and with a gap above the substrate as illustrated in Figure 22. Sapphire as non-porous alumina has been chosen due to its high transmittance in the near infrared (NIR) and its high emittance in the long-wavelength infrared (LWIR). The spectral transmittance of sapphire is additionally depicted in Figure 22. The measurements have been performed with two radiation thermometers which are sensitive at 1 µm (NIR-pyrometer) and 10 µm (LWIR-pyrometer), respectively. At a wavelength of 1 µm mainly transmitted radiation from the substrate is detected by the NIR-pyrometer whereas at a wavelength of 10 µm only radiation from the sapphire surface is detected by the LWIR-pyrometer.

The substrate has been heated up to temperatures of 900 K and 1500 K and the temperatures of the substrate and the sapphire surface have been determined using the NIR- and LWIR-pyrometer. The detected temperatures of the sapphire surfaces for the two cases (without and with gap) are shown in Figure 22. The temperature of the sapphire sample without gap is significantly higher than the temperature of the sapphire sample with gap as the gap increases the thermal contact resistance.

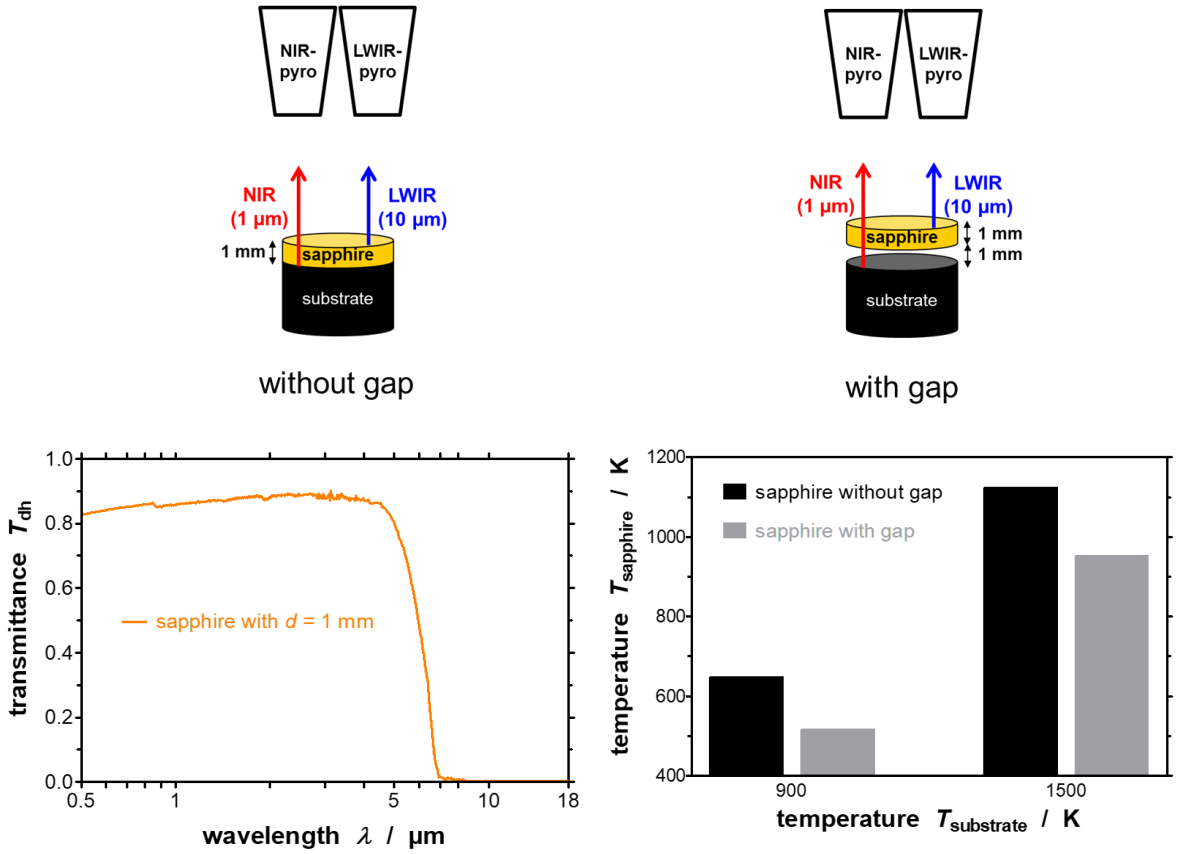

Figure 22 - Detected temperatures of the sapphire surface versus the temperature of the substrate for two cases: sapphire without gap and sapphire with gap. Additionally, the spectral directional-hemispherical transmittance of the sapphire sample is shown.

c) Validation of the measurement capabilities for determining the effective thermal contact resistance

For determining the thermal contact resistance and the mechanical adhesion of coatings to the substrate and accordingly potential delaminations, a non-invasively and contactless testing method has been developed at ZAE Bayern and FHWS, which implements a thermographic camera and a laser. Hence, the setup principally consists of two main components, which are illustrated in Figure 23:

- a laser, which serves as energy source for applying heat into the coating and
- a thermographic camera, which measures the lateral temperature distribution across the surface of the coating.

For performing the measurement, a short laser pulse heats up the surface of the coating (e.g. a thermal barrier coating, TBC) and the heat propagation into the TBC and further on from the TBC into the substrate is detected by a thermographic camera. This procedure is also known as active thermography. The surface temperature of the TBC locally increases at positions where an increased thermal contact resistance occurs, which hinders the thermal flow into the substrate. As partial delamination of the TBC is usually correlated with an increased thermal contact resistance, this method is suitable to detect partial delaminations, especially if the delamination is not yet optically perceivable. In the laboratory setup, the whole sample can be thermalized up to a defined temperature using an induction heater.

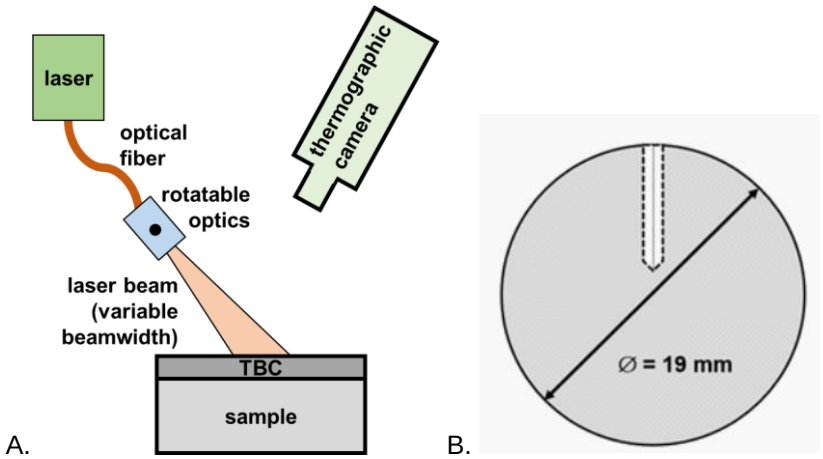

Figure 23 - (A.) Scheme of the developed method for non-contact and non-destructive testing (NTD) of layered systems with active thermography using a laser and a thermographic camera at ZAE Bayern and FHWS. (B.) Sketch of the test specimen used by FHWS.

For testing the setup at ZAE Bayern, specimens with defined partial delamination have been prepared by atmospheric plasma spraying (APS). For creating an air gap with a certain geometry (e.g. a line as shown in Figure 24 top left) between the substrate and the TBC, at first a bond coat was only applied onto the grey areas of the discoidal substrate in Figure 24 (top left) leaving the white area uncoated. Afterwards the TBC was applied onto the whole area of the substrate. Finally, the specimen, which consists of substrate, partial bond coat and TBC topcoat, was annealed at 800 °C for 2 h. As a result of the annealing, an air gap occurred between the substrate and the TBC in the areas without bond coat. This is due to the fact, that the adhesion of the TBC to the bond coat is strong, whereas the adhesion of the TBC to the substrate is weak.

Despite this partial delamination, the TBC is intact, and no damage is visible when looking at the TBC surface. Hence, on a photograph of the TBC-surface (Figure 24 top right) no delamination can be seen. However, the partial delamination can be detected and visualized by performing the above-mentioned non-destructive test.

A collection of selected thermographic images, which have been generated during the heating and the cooling period, is shown at the bottom of Figure 24. On the first picture, no structure is visible as all surfaces exhibit the same temperature. After heating the sample by the laser, the surface temperature increases. The temperature rise is significantly higher at the position of the air gap, compared with the temperature rise at other positions without air gap.

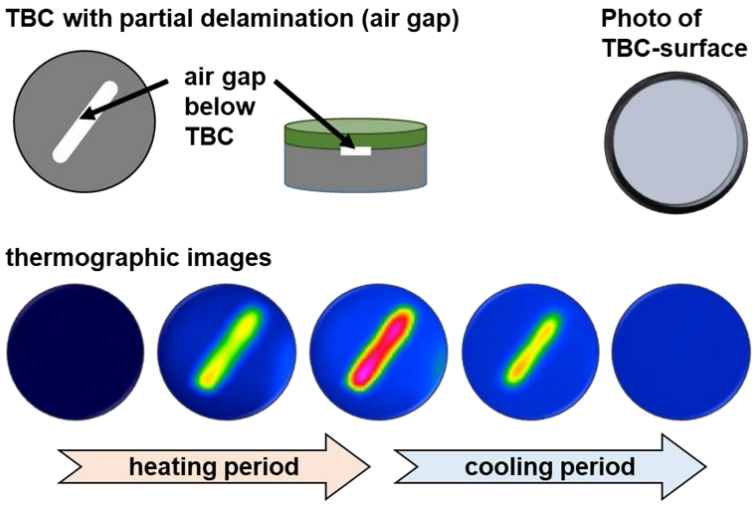

Figure 24 - Thermal barrier coating (TBC) on steel substrate with defined partial delamination (top left) and temperature distributions on the coating surface determined by active thermography during the heating and cooling phase (bottom). No delamination is visible on a photo of the coating surface (top right).

As previously explained the heat load is efficiently dissipated onto the substrate if a strong adhesion and therefore a low thermal contact resistance exists. However, the air gap acts as a thermal resistance and reduces the heat flow onto the substrate and thus the dissipation of the heat input, which leads to a locally higher surface temperature at the position of the air gap. After turning the laser off, the surface temperature decreases and finally the differences in temperature disappear, with the surface temperature at the end is slightly higher than at the beginning.

For the quantitative description of the experiment as shown in Figure 23 (B.), FHWS developed a numerical simulation using COMSOL with comparable parameters. In the simulation, ZrO_2 has been used as thermal barrier coating and the heat was applied on the front side by a laser pulse (τ= 0.1 ms, Q_{laser} = 1 J, and D_{beam} = D_{sample}). As shown in Figure 25, on the front side of the sample's surface one can see the temperature profile along the sectional axis after heating starting from point A to B on the left side, where the inhomogeneity (= contact resistance between the layers) on the left side of the sample (point A) is very clearly indicated. The maximum calculated temperature difference along the diameter (A to B) is around 2.5 K.

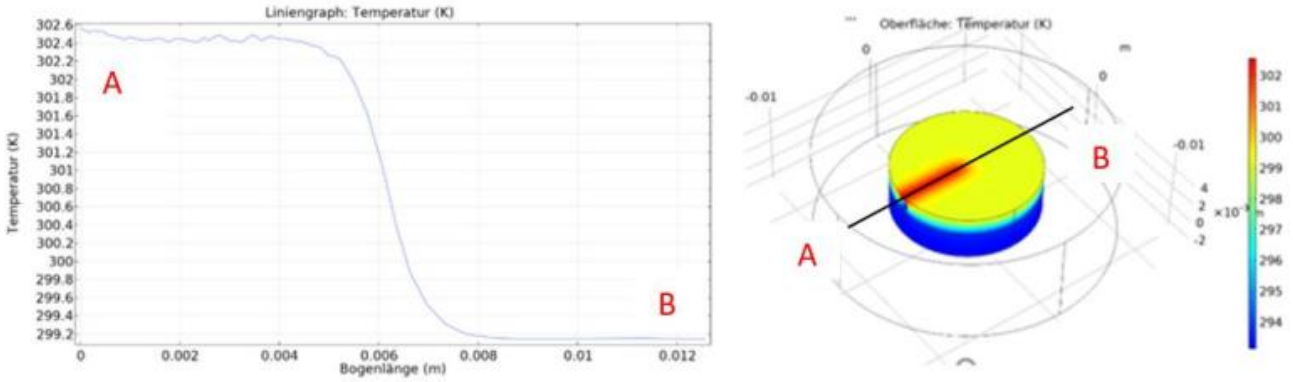

Figure 25 - Simulation of the preliminary experiment with COMSOL Multiphysics®.

4.4.2 Development of a model for thermal contact resistance for de-bonding

NPL further developed their model for parameter estimation from laser flash experimental data of multi-layered specimens. The main development is that the interfaces between the layers may now be partially or fully debonded. The new development is an inverse model that simulates a laser flash thermal diffusivity measurement on a sample consisting of two or three layers that may have partial debonds between the layers to determine unknown parameters associated with the partially debonded regions and/or heat transfer coefficients by matching model results to measured data obtained by a thermogram, and potentially additional thermal images.

The inverse model has been compiled into executable software called Opt3LDB. The software and the user manual are available in the Hi-TRACE project Share Point. If thermal images are used in the objective function, then the software also provides an estimate of the laser power density. The user of the software is able to specify initial estimates of the parameters of interest. The success of the optimisation is strongly dependent on the starting point of the optimisation; this is unavoidable and is the nature of optimisation. The inverse model Opt3LDB has been used to calculate the bond quality and heat transfer coefficient of multi-layer artefacts, both the IG210 graphite/Hf/IG210 graphite system and the SiC/Mo/SiC system.

4.4.3 Development of high-temperature multi-layer laser flash artefacts

Two material systems of high-temperature multi-layer LFA artefacts with and without defined debonds were created and characterised: IG210 graphite/Hf/IG210 graphite, and SiC/Mo/SiC.

The IG210 graphite/Hf/IG210 graphite system theoretically has the potential to be an artefact that can be used as reference at very high temperatures, i.e. above 2000 °C. The production of the 1st batch of the IG210 graphite/Hf/IG210 graphite artefacts was shown to be reproducible, with the defect regions being consistent, circular, and centred. The SAM images are as shown in Figure 26. The LFA thermal curves, as shown in Figure 27, were consistent between artefacts of the same type, indicating good uniformity among the artefacts.

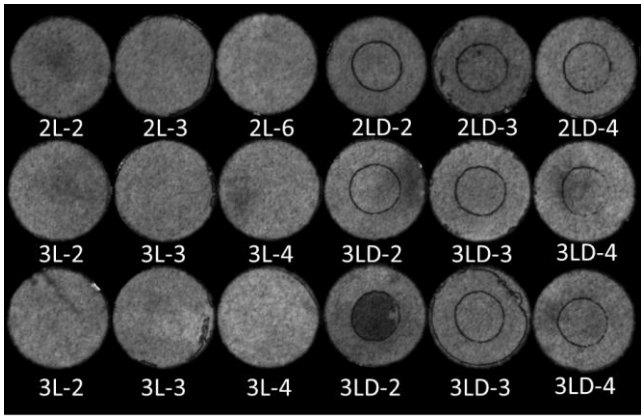

Figure 26 - SAM images of multi-layer graphite LFA artefacts with a hafnium carbide interface. Row 1 corresponds to the interface of bi-layer artefacts. Rows 2 and 3 correspond respectively to interface 1 and 2 of the tri-layer artefacts. Item numbers prefixed with '2L' are bilayer, prefix '3L' are tri-layer. 'D' corresponds with a circular central defect being present.

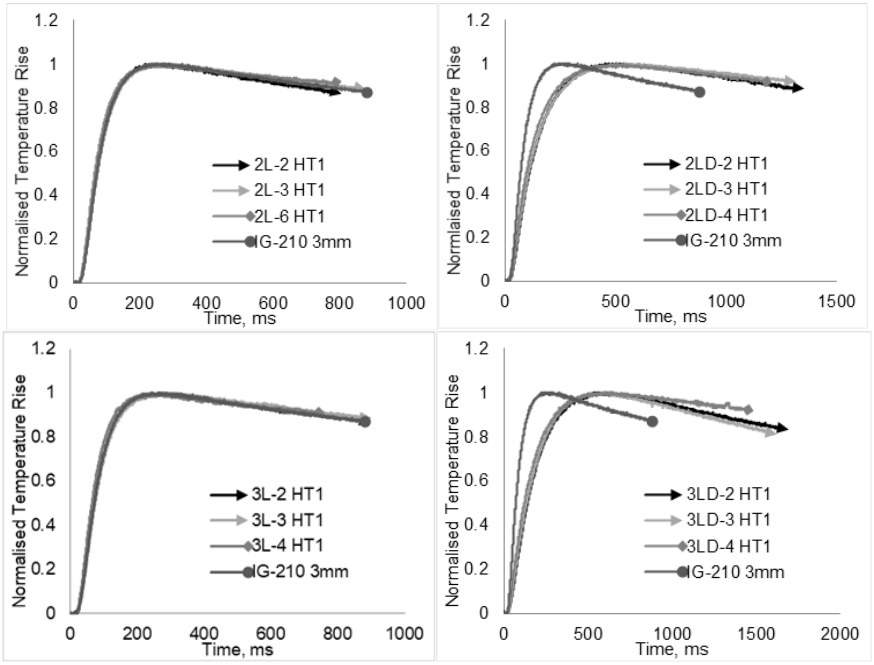

Figure 27 - LFA thermal curves of multi-layer graphite / hafnium carbide artefacts at 1000 °C compared to a 3 mm monolayer of IG-210 grade graphite.

The thermal stability was also investigated, and all artefacts were shown to be stable for at least two or three thermal cycles, which is considered to be sufficient for use in the intercomparisons in the objective 4 of the project. However, using SPS process it was found problematic to reproducibly manufacture further batches of the IG210 graphite/Hf/IG210 graphite artefacts for use in intercomparison.

4.4.4 Uncertainty analysis of the models and methods

NPL developed software to evaluate the uncertainties associated with the outputs of the inverse model for bond quality, UncOpt3LDB. It uses the Latin hypercube sampling method to evaluate the uncertainties associated with the bond quality parameters and heat transfer coefficients. Based on the sensitivity study results, the software allows the following parameters to be defined as uncertain: thermal conductivity of any layer; specific heat capacity of any layer; density of any layer; and either semi-axis of the ellipse on either interface which defines the debonded region. Any combination of parameters can be treated as uncertain. Each uncertain parameter can be assigned either a uniform distribution or a Gaussian distribution.

The results of each individual optimisation run are written to file for future use. The calculated bond quality and heat transfer coefficient values are used to estimate the full covariance matrix, and hence uncertainty associated with each parameter. An example is given on using the uncertainty evaluation software to estimate the uncertainty of the deduced bond quality and heat transfer coefficient for a three layer IG210 graphite/Hf/IG210 graphite/Hf/IG210 graphite specimen with a 6 mm diameter defect at the centre of each of the two Hf foil layers. However, it is not possible to state whether these values are typical for the experiment because they are a single example with a small sample size. The correlation between each pair of unknown quantities was greater than 0.99, suggesting that the outputs of the inverse process are strongly correlated for this set of input values.

Intercomparisons were carried out using the IG210 graphite/Hf/IG210 graphite artefacts. The results of the intercomparison up to 1200 °C have been analysed for the data from NPL, FHWS and LNE (up to 800 °C), respectively. The deduced bond quality for the defect region of sample 2LD-3 measured by NPL and that of sample 2LD-2 measured by FHWS agree to within 16 % at 1200 °C, and 12 % at 1000 °C. The deduced bond quality for the defect region of sample 3LD-4 measured by NPL and that of sample 3LD-1 measured by FHWS agree to within 43 % at 1000 °C. The 43 % difference might be caused by the difference in the samples, the quality of the measured LFA thermograms, and quality of the fitted curves.

4.4.5 Application of the methods at high temperatures

a) quantification of mechanical adhesion (i.e. state of bonding)

The quantification of mechanical adhesion (i.e. state of bonding) of the multi-layered IG210 graphite/Hf/IG210 graphite specimens was investigated using two approaches.

The 1st approach is via comparing the SAM images and bond quality (i.e. thermal interface conductance) between the fresh samples with or without introduced defect region at the centre. As seen in Figure 26, SAM images of samples 2LD and 3LD clearly show the introduced circular defect region at the centre of each sample. The curves in Figure 27 and the half-rise time have shown the significant slowdown of the temperature rise at the rear face of the specimens. The deduced bond quality values for the defect region of samples 2LD-3, 2LD-4 and 3LD-4 are in the order of 10^4 W m^{-2} K^{-1}, while the bond quality values for the bonded region of these specimens are in the order of 10^{10} W m^{-2} K^{-1}. In other words, there are significant differences in the bond quality values between the bonded region and de-bonded region, and they are clearly detected by LFA and imaged using SAM.

The second approach is via comparing the microstructure change at the interface layers, and the bond quality (i.e. thermal interface conductance) change between fresh sample and thermally cycled sample. A comparison between a fresh sample and sample 2L-6 after the 5th thermal cycle can be seen in

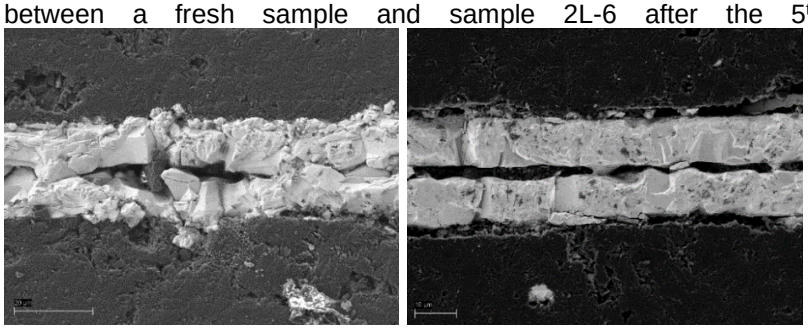

Figure 28. There is a void centrally along the interface of the hafnium-carbide layer in both fresh and cycled samples, and this void line thickened after thermal cycling. As a result, the bond quality (i.e. thermal interface conductance) changed by 7 orders of magnitude. The bond quality of sample 2L-6 changed from 10^{12} W m^{-2} K^{-1} after the 1st thermal cycle to 10^5 W m^{-2} K^{-1} after the 5th thermal cycle.

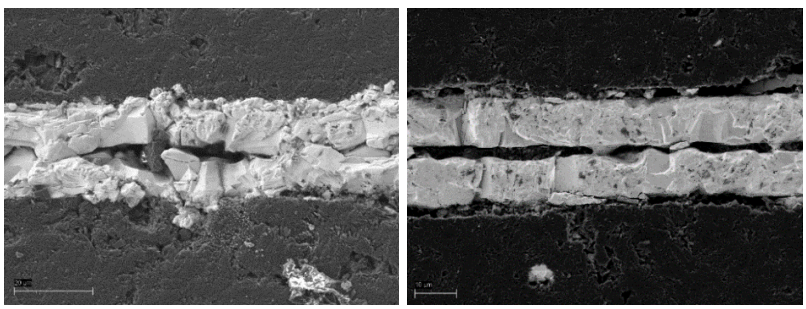

Figure 28 - Secondary electron SEM images for fresh bi-layer IG210 graphite/Hf/IG210 graphite sample (left) and sample 2L-6 after heat cycled five times (right).

b) Metallic layer bonded silicon carbide - SiC/Mo/SiC system

Metallic layer bonded silicon carbide is a promising material system for nuclear structural application. In this project, the thermal interface conductance or bond quality of SPS jointed SiC/Mo/SiC multi-layer system has been investigated. Samples have been characterised and have shown acoustic and thermal consistency. They are thermally stable to at least 5 heat cycles, see Figure 29. The interface microstructure is very consistent.

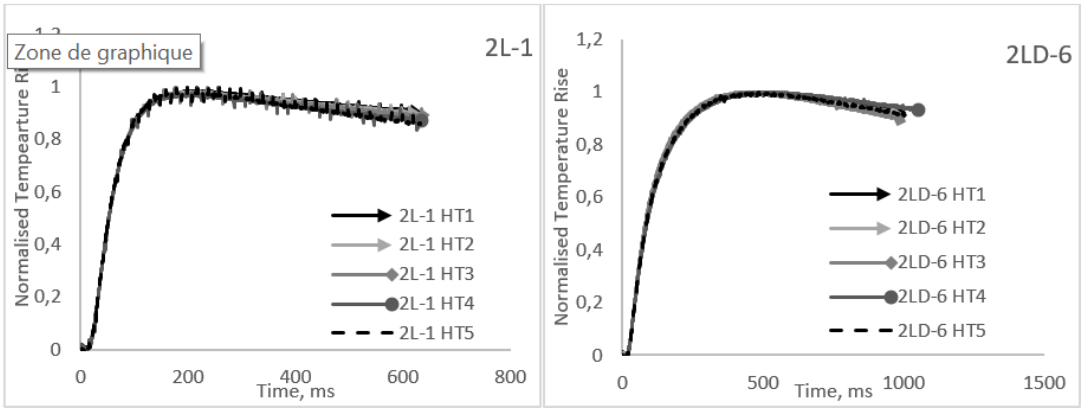

Figure 29 - LFA Thermograms of SiC/Mo/SiC artefacts 2L-1 (left) and 2LD-6 (right) at 1000 °C, after the 1st, 2nd, 3rd, 4th, and 5th thermal cycle.

Intercomparisons were carried out using the SiC/Mo/SiC artefacts. The results of the intercomparison up to 1200 °C have been analysed for the data from NPL, FHWS and LNE (up to 800 °C), respectively. The deduced bond quality for the defect region of sample 2LD-6 measured by NPL and that of sample 2LD-5 measured by FHWS agree to within 28 % at 1200 °C, and 26 % at 1000 °C. The difference might be caused by the difference in the samples, the quality of the measured LFA thermograms, and quality of the fitted curves.

In summary, The SiC/Mo/SiC system has shown excellent potential to become a high temperature LFA reference artefact.

4.4.6 Conclusion

FHWS has adapted a laser flash set-up to measure the thermal contact resistance in multilayer systems from simultaneous temperature measurements of the front and back side of the test specimen. Subsequently, the thermal contact resistances of different layer systems have been measured at FHWS using the spectroscopic values determined at ZAE Bayern as input. NPL has further developed and validated an inverse heat transfer model for laser-flash measurements and developed software to evaluate the uncertainties associated with the bond quality parameters and heat transfer coefficients. The inverse model has been used to extract the thermal interface resistance of bi-layer and tri-layer material systems from thermograms obtained during these laser flash experiments. It has been designed to allow setting the thermal interface resistance of the de-bonded region and that of the rest of the interface area to different values.

FHWS and ZAE have customised a procedure to calibrate the adapted LFA facility with samples of thermal barrier coating, e.g. plasma-spray partially-yttria (Y_2O_3) stabilized zirconia (PYSZ) and alumina coatings above 1000 °C. Furthermore, a setup for performing thermal imaging measurements was developed and applied on layered systems. It was shown that this set-up can successfully detect partial delamination underneath thermal barrier coatings.

NPL has characterised bi-layer and tri-layer systems (composed of IG210 graphite layers and metal foil bonds, or SiC layers and Mo foil) with and without a defect region at the centre. The quality of the bonded systems has been checked non-destructively by using a scanning acoustic microscope (SAM), and destructively by using scanning electron microscope (SEM) to examine the microstructure at the bonded / de-bonded regions. The IG210 graphite/Hf foil/IG210 graphite system theoretically has the potential to become an artefact that could be used as reference above 2000 °C. However, using the spark plasma sintering (SPS) process it was found problematic to reproducibly manufacture reproducible batches of this artefact. In addition, they also showed limited thermal cycle life due to the mechanical instability of graphite. However, the SiC/Mo/SiC systems showed excellent potential to become a high temperature LFA reference artefact, although limited to 1600 °C.

LFA measurements have been carried out up to 1200 °C by NPL, FHWS, and LNE on the artefacts of the two bi-material systems and the experimental curves (thermograms) have been analysed by NPL. The inverse heat transfer model has been applied to calculate the interface thermal resistance, i.e. the bond quality, of these layered specimens (with and without defects) from the LFA thermograms. Measurements on samples with dedicated defects have been also performed with the set-up based on thermal imaging to find a validated approach for detection of mechanical de-bonding.

The objective was successfully achieved. The quantification of mechanical adhesion (i.e. state of bonding) was investigated using these two approaches.

5 Impact

The activities and results of the Hi-TRACE project have been presented through 20 contributions (oral presentations or posters) at national and international conferences, as well as in eight articles published in open access scientific peer-reviewed journals. An article describing the project has been also published in a trade journal of the nuclear energy industry. Three additional papers have been written: two are non-open access and another one has been drafted. The latter one will be open access.

A one-day workshop was held online on January 2021 with about 40 attendees. The industrial needs, the main achievements and the results obtained were presented, and a virtual tour of the laboratories of the organizing partner with demonstrations was also included.

To ensure the project activities remain aligned with stakeholder needs, the consortium has built up a stakeholder advisory board composed of ten members coming from industry and scientific community. It provided feedback on the work of the consortium, the results from the project activities and gave advice on the “industrial” materials to be studied.

Impact on industrial and other user communities

The main industrial areas that may directly benefit from the outputs were involved in the project as stakeholders: aerospace and nuclear industries, and manufacturers of measurement instruments. They are all equipped with facilities to measure high temperature thermal properties and their proximity with the consortium enables an early exploitation and adoption of the outputs.

Thanks to the network of reference facilities developed during the project, the European industrial community can benefit from reliable and traceable thermophysical properties data at high temperatures. New commercial offers of calibration and test services about thermophysical properties measurements up to 3000 °C are proposed by the partners (in particular for thermal diffusivity and specific heat) and have already been applied to specific demands coming from space and metallurgy industries.

The reference laser flash apparatus improved during the project participated in a “feasibility study” to demonstrate to the European space industries and agencies its capability to measure thermal diffusivity of advanced materials at very high temperatures.

A series of five e-learning modules related to the high-temperature thermal diffusivity measurements by the laser flash method and to the assessment of associated uncertainties have been prepared for users of LFA. These tutorials are now available in the Zenodo open access repository, and on the project website.

Three refractory materials (isotropic graphite, tungsten and molybdenum) were studied via inter-laboratory comparisons on thermal diffusivity, specific heat and emissivity measurements. The results obtained during the project do not enable to finally decide if they can be potential reference materials for calibration of calorimeters and emissivity devices. In contrast, it seems that they could be proposed as candidate reference materials for thermal diffusivity measurements, provided that additional tests would be done in terms of long-term stability. Datasets with thermal diffusivity, specific heat, and spectral emissivity values of these three materials versus temperature have been uploaded in the Zenodo open access repository.

Impact on the metrology and scientific communities

Based on the project’s results, a good practice guide for measurement of thermal diffusivity up to 3000 °C by the laser flash method was prepared. This guide contains information about requirements on specimens and facilities, measurement methodology and data analysis in order to obtain the proper thermal diffusivity values. It has been identified by the WG Best practice of the EURAMET TC-T (Technical Committee for Thermometry)

as a document that will serve as strong basis for a EURAMET guideline currently under construction on that topic. After approval, it will be made available on the EURAMET website.

A specific training session related to thermophysical properties measurements has been provided to young researchers coming from National Metrology Institutes (NMIs) and Designated Institutes (DIs) from Turkey, Slovakia, Greece, Bosnia & Herzegovina, Serbia, Italy during the Thermal metrology Summer School organized by EURAMET TC-T end of 2018.

A proposal related to the organisation of an inter-laboratory comparison on thermal diffusivity measurement of high conductive materials by the laser flash method has been submitted by the Thermophysical Quantities Working Group (chaired by the coordinator of the Hi-TRACE project) of the TC-T. It was approved by TC-T in April 2021 and registered as EURAMET project 1524. Three partners are involved in this exercise, which is an essential preliminary step to propose new Calibration and Measurement *Capabilities* (*CMC*) in that field.

Thanks to the experience gained in this project and to a higher visibility, several partners have been contacted by new consortia to participate in two European joint research projects related to the measurement of thermal properties at very high temperatures.

Impact on relevant standards

Discussions have been initiated with relevant national and international standardization bodies on potential impacts of the project on standards dealing with “advanced ceramics”.

An informative annex about the precision of the laser flash method and the uncertainty associated with thermal diffusivity measurements has been prepared and submitted to the ISO TC206 WG7 “Monolithic ceramics - physical and thermal properties” for addition in the ISO 18755 standard “Fine ceramics (advanced ceramics, advanced technical ceramics) - Determination of thermal diffusivity of monolithic ceramics by laser flash method”. It is anticipated that the final version of the ISO 18755 standard with this annex will be examined for publication in 2022.

A discussion should be engaged in the second half of 2022 at the CEN/TC 184 SC1 “Advanced technical ceramics - Composite ceramics” to replace the current EN821-2 “Monolithic ceramics - Thermo-physical properties - Part 2: Determination of thermal diffusivity by the laser flash (or heat pulse) method” by the new version of the ISO 18755 standard.

In the near future, the outcomes of the project 17IND11 Hi-TRACE could be used for the revision of the EN ISO 19629 “Fine Ceramics (advanced ceramics, advanced technical ceramics) - Thermophysical properties of ceramic composites - Determination of unidimensional thermal diffusivity by flash method” and EN ISO 19628 “Fine Ceramics (advanced ceramics, advanced technical ceramics) - Thermophysical properties of ceramic composites - Determination of specific heat capacity” standards in 2023 and 2026.

These actions will be done via the participation of three partners of the Hi-TRACE project in the concerned standardization committees as members or chairs of subcommittees.

Longer-term economic, social and environmental impacts

Compared to the usual industrial sectors, space and nuclear industries work with long-term projects (typically 10 to 20 years), with many steps of modelling and test for optimizing their processes and devices, especially in terms of safety and reliability. The metrological facilities developed in this project enables a full characterisation (thermal diffusivity, specific heat, emissivity, temperature of fusion) of the advanced materials used in these industries in conditions close to that encountered in their real applications.

More accurate high temperature thermophysical properties data will increase the reliability of the thermal behaviour prediction of these materials in critical conditions. This will help the concerned European industries in optimizing the modelling and test steps and in reducing the corresponding costs.

The aeronautics sector will benefit from using new experimental tools and models of thermal contact resistance measurements in evaluating the progress of ablation phenomena. It may contribute, for example, to the reduction of space module weight, the sustainability of refractories and the extension of gas turbine lifetime thus reducing waste.

6 List of publications

Eber A., Pichler P. and Pottlacher G., Re-investigation of the normal spectral emissivity at 684.5 nm of solid and liquid molybdenum. *Int J Thermophys* **42,** 17 (2021). https://doi.org/10.1007/s10765-020-02769-7

Milošević N., Application of the subsecond calorimetry technique with both contact and radiance temperature measurements: case study on solid phase tungsten at very high temperatures. *J Therm Anal Calorim* (2021). https://doi.org/10.1007/s10973-021-10866-4

Failleau G., Fleurence N., Beaumont O., Razouk R., Hameury J. and Hay B., Metal-carbon eutectic high temperature fixed points for in-situ calibration of radiation thermometers, High Temp High Press **50**, 149 (2021). 10.32908/hthp.v50.1013

Razouk R., Beaumont O., Hameury J. and Hay B., Towards accurate measurements of specific heat of solids by drop calorimetry up to 3000 °C. Therm Sci Eng Prog **26**, 101130 (2021) https://doi.org/10.1016/j.tsep.2021.101130

*Arduini M., Manara J., Stark T., Ebert H.-P. and Hartmann J., Development and evaluation of an improved apparatus for measuring the emissivity at high temperatures, Sensors **21**,* 6252 (2021). https://doi.org/10.3390/s21186252

Hay B., Beaumont O., Failleau G., Fleurence N., Grelard M., Razouk R., Davée G. and Hameury J., Uncertainty assessment for very high temperature thermal diffusivity measurements on molybdenum, tungsten and isotropic graphite. *Int J Thermophys* **43,** 2 (2022). https://doi.org/10.1007/s10765-021-02926-6

Farooqui A., Morrell R., Wu J., Wright L., Hay B., Pekris M., Whiting M.J. and Saunders T., Development of high temperature multi-Layer laser flash artefacts. *Int J Thermophys* **43**, 13 (2022). https://doi.org/10.1007/s10765-021-02928-4

Urban D., Anhalt K., Dynamic measurement of specific heat above 1000 K. *Int J Thermophys* **43**, 77 (2022). https://doi.org/10.1007/s10765-022-03005-0